AIMS Mathematics, 11(4): 11776–11809.
DOI:10.3934/math.2026485
Received: 07 February 2026
Revised: 09 April 2026
Accepted: 22 April 2026
Published: 28 April 2026

https://www.aimspress.com/journal/Math

Research article

Mathematical analysis of hepatitis C virus transmission with awareness, testing, and treatment interventions

Debnarayan Khatua[1,2], **Bapin Mondal**[1,*], **Md Sadikur Rahman**[3] **and Sadiah M. Aljeddani**[4,*]

[1] Department of Mathematics, School of Computer Science and Artificial Intelligence, SR University, Warangal, Telangana, 506371, India
[2] Department of Applied Science and Humanities, Parul Institute of Technology, Parul University, Vadodara, Gujarat 391760, India
[3] Department of Mathematics, Khalisani Mahavidyalaya, Chandannagar, Hooghly-712138, West Bengal, India
[4] Mathematics Department, Al-Lith University College, Al-Lith 21961, Umm Al-Qura University, Makkah, Saudi Arabia

* **Correspondence:** Email: bapinmondal1@gmail.com, smgadany@uqu.edu.sa.

Abstract: This study introduces a deterministic compartmental model of hepatitis C virus (HCV) transmission with behavioral awareness, diagnosis tests, and treatment interventions as control strategies. The study evaluates the autonomous fixed-control system to determine its basic reproduction number ($\mathcal{R}_0$), which enables the description of its equilibrium points and an analysis of its stability and bifurcation patterns. The study considers the local asymptotic stability of the disease-free equilibrium when $\mathcal{R}_0 < 1$, and finds at least one endemic equilibrium when $\mathcal{R}_0 > 1$. The local stability of the endemic equilibrium is assessed using the Routh-Hurwitz conditions, whereas global asymptotic stability is established under additional assumptions, including no disease-induced mortality and the uniqueness of the endemic state. Using the theory of the center manifold, it was subsequently proven that the model goes through a forward transcritical bifurcation when $\mathcal{R}_0 = 1$. Sensitivity analysis performed at the local level and also with Latin hypercube sampling–partial rank correlation coefficient analysis showed that both diagnostic testing and behavior awareness are the most effective interventions to reduce transmission, while treatment primarily reduces disease prevalence and its burden. The analytical results are verified through numerical simulations, which strongly emphasize the importance of integrating intervention strategies to improve HCV control.

Keywords: hepatitis C virus; mathematical epidemiology; compartmental model; awareness and testing interventions; stability analysis; sensitivity and PRCC analysis
Mathematics Subject Classification: 37G35, 37N25

1. Introduction

Hepatitis C virus (HCV) infection remains a major global health burden despite the availability of highly effective direct-acting antivirals (DAAs). The World Health Organization (WHO) estimates that around 50 million people live with chronic HCV infection and that about one million new infections occur each year, with diagnosis and treatment coverage still inadequate in many settings [1–3]. In 2016, the WHO set elimination goals for 2030, including significant reductions in incidence and HCV-related mortality, which motivated increased efforts in screening, linkage to care, and scale of treatment [4–6].

Recent clinical and public-health syntheses emphasize that elimination is technically feasible but programmatically challenging, particularly because transmission persists in key populations, reinfection remains possible, and losses occur along the testing-to-treatment cascade [5,7,8]. Empirical and modeling work increasingly highlights the importance of simplifying diagnostic pathways (e.g., single-visit testing and point-of-care RNA strategies), decentralizing services, and expanding nonspecialist prescribing to improve uptake and reduce ongoing transmission [9, 10].

Mathematical models offer a principled approach to quantifying the combined impact of prevention, awareness, diagnosis, and treatment interventions, and to identify threshold conditions for elimination [11–13]. For people who inject drugs (PWID) and other high-risk networks, dynamic transmission modeling and empirical analyzes show that treatment scale-up must be coupled with sustained harm-reduction and repeated tests to achieve and maintain incidence reductions [14–16]. Cost-effectiveness studies similarly conclude that intensified testing and treatment strategies can be efficient and may accelerate progress toward elimination targets when implemented at scale [10, 17].

With the perceived gap, we formulate a deterministic compartment model for HCV transmission that incorporates behavioral awareness, diagnostic testing, and treatment intervention in a complete model. The main contribution of this research study is the practical results presented alongside its structural framework. We develop an HCV transmission model which divides susceptible people into two groups of aware and unaware individuals to show how awareness influences their effective exposure rates instead of being included in the transmission coefficient. The model connects three intervention components in a mechanistic order: awareness that changes risk levels, testing for undiagnosed cases, and treatment, which decreases hospitalizations and recovery needs. The integrated framework enables us to use standard epidemic-analysis tools for threshold behavior identification while we measure how different intervention methods affect disease transmission and total disease burden. The model is shown to be well-posed, and the basic reproduction number is derived using the next-generation approach [18]. To characterize threshold dynamics and possible bifurcation behavior near $\mathcal{R}_0 = 1$, we employ center-manifold arguments [19]. Finally, we quantify the relative influence of epidemiological and intervention parameters using global uncertainty and sensitivity tools (e.g., LHS/PRCC), which support policy-relevant prioritization of integrated HCV control strategies [20, 21].

2. Model formulation

We consider a deterministic compartmental model to describe the transmission dynamics of HCV in a heterogeneous population that incorporates awareness, diagnosis, and treatment interventions. The total population at time t, denoted by $N(t)$, is subdivided into six mutually exclusive compartments:

$$N(t) = S_1(t) + S_2(t) + U(t) + I(t) + H(t) + R(t),$$

where S_1 represents unaware susceptible individuals, S_2 denotes aware susceptible individuals, U denotes unidentified infected individuals, I represents identified infected individuals, H corresponds to hospitalized individuals undergoing treatment, and R denotes recovered individuals. The variables of the model state and the biological interpretations are summarized in Table 1, while the parameter definitions and control descriptions are provided in Table 2.

Table 1. Description of state variables of the HCV transmission model.

Variable	Biological description
$S_1(t)$	Susceptible individuals unaware of HCV infection
$S_2(t)$	Susceptible individuals aware of HCV infection
$U(t)$	Unidentified (undiagnosed) HCV-infected individuals
$I(t)$	Identified (diagnosed) HCV-infected individuals
$H(t)$	Hospitalized HCV-infected individuals under treatment
$R(t)$	Recovered individuals with temporary immunity
$N(t)$	Total population size, $N = S_1 + S_2 + U + I + H + R$

Table 2. Model parameters and control variables with biological interpretation.

Parameter	Description	Unit
A	Recruitment rate into susceptible population	persons $\cdot$ time^{-1}
β_1	Effective contact rate for unaware susceptibles	time^{-1}
β_2	Effective contact rate for aware susceptibles	time^{-1}
ε	Modification factor for infectiousness of identified individuals	dimensionless
δ	Natural death rate	time^{-1}
ξ_1	Natural recovery rate of infected individuals	time^{-1}
γ_1	Hospitalization rate of identified infected individuals	time^{-1}
η_1	Disease-induced death rate of identified infected individuals	time^{-1}
η_2	Disease-induced death rate of hospitalized individuals	time^{-1}
τ_1	Diagnosis (testing) rate of unidentified infected individuals	time^{-1}
τ_2	Treatment-induced recovery rate of hospitalized individuals	time^{-1}
α_1	Force of infection for unaware susceptible people	time^{-1}
α_2	Force of infection for aware susceptible people	time^{-1}
$u_1(t)$	Media awareness control effort	$0 \leq u_1 \leq 1$
$u_2(t)$	Diagnostic testing control effort	$0 \leq u_2 \leq 1$
$u_3(t)$	Treatment control effort	$0 \leq u_3 \leq 1$

The dynamics of the population is governed by the following system of ordinary differential equations [22]:

$$\begin{aligned}
\frac{dS_1}{dt} &= A - \alpha_1 S_1 - \beta_1 u_1 S_1 + \beta_2(1-u_1)S_2 - \delta S_1,\\
\frac{dS_2}{dt} &= \beta_1 u_1 S_1 - \beta_2(1-u_1)S_2 - \alpha_2 S_2 - \delta S_2,\\
\frac{dU}{dt} &= \alpha_1 S_1 + \alpha_2 S_2 - \tau_1 u_2 U - (\xi_1 + \delta)U,\\
\frac{dI}{dt} &= \tau_1 u_2 U - (\gamma_1 + \eta_1 + \xi_1 + \delta)I,\\
\frac{dH}{dt} &= \gamma_1 I - (\tau_2 u_3 + \eta_2 + \delta)H,\\
\frac{dR}{dt} &= \xi_1(U + I) + \tau_2 u_3 H - \delta R,
\end{aligned} \tag{2.1}$$

where the forces of infection are defined as

$$\alpha_1 = \frac{\beta_1(U + \varepsilon I)}{N}, \qquad \alpha_2 = \frac{\beta_2(U + \varepsilon I)}{N}.$$

The time-dependent control variables $u_1(t)$, $u_2(t)$, and $u_3(t)$ represent media awareness campaigns, diagnostic testing efforts, and treatment interventions, respectively, satisfying

$$0 \le u_i(t) \le 1, \quad i = 1, 2, 3.$$

All parameters are assumed to be non-negative and biologically meaningful.

We introduced intervention variables $u_1(t)$, $u_2(t)$, and $u_3(t)$ in our study through general time-dependent expressions to show how awareness and testing and treatment efforts could change. The analytical results, developed in Sections 4–8 of the study, were obtained from the autonomous model, which maintains its controls at fixed, permanent values or at permanent average intervention levels. The standard reduction method establishes clear definitions for equilibrium states, threshold points, and bifurcation concepts. All formal results about $\mathcal{R}_0$, equilibria, and stability control the constant-control model, whereas later policy interpretations use qualitative methods to compare fixed control levels with exploratory numerical scenarios.

3. Well-posedness analysis

3.1. Positivity of solutions

Theorem 1. *For any non-negative initial conditions,*

$$S_1(0), S_2(0), U(0), I(0), H(0), R(0) \ge 0,$$

the solutions of system (2.1) *remain non-negative for all* $t > 0$.

Proof. Consider the first equation of (2.1). At $S_1 = 0$,

$$\left.\frac{dS_1}{dt}\right|_{S_1=0} = A + \beta_2(1-u_1)S_2 \ge 0.$$

Similarly, evaluating each equation on the corresponding boundary hyperplanes yields non-negative derivatives. Since the right-hand side of the system (2.1) is locally Lipschitz continuous, solutions exist and are unique, and the positive orthant $\mathbb{R}^6_+$ is forward invariant. Hence, all state variables remain non-negative for all $t > 0$. □

3.2. Boundedness and invariant region

Theorem 2. *All solutions of system* (2.1) *are uniformly bounded in the region*

$$\Omega = \left\{(S_1, S_2, U, I, H, R) \in \mathbb{R}^6_+ : \ N(t) \leq \frac{A}{\delta}\right\}.$$

Proof. Summing all equations of the system (2.1) yields

$$\frac{dN}{dt} = A - \delta N - \eta_1 I - \eta_2 H \leq A - \delta N.$$

Solving the differential inequality gives

$$N(t) \leq \frac{A}{\delta} + \left(N(0) - \frac{A}{\delta}\right) e^{-\delta t}.$$

Thus, $N(t)$ is bounded above by A/δ for all $t > 0$. Hence, Ω is positively invariant. □

4. Equilibria of the model

In this section, we characterize the steady states of system (2.1). An equilibrium $\mathcal{E} = (S_1, S_2, U, I, H, R)$ satisfies

$$\frac{dS_1}{dt} = \frac{dS_2}{dt} = \frac{dU}{dt} = \frac{dI}{dt} = \frac{dH}{dt} = \frac{dR}{dt} = 0.$$

Recall the forces of infection

$$\alpha_1 = \frac{\beta_1(U + \varepsilon I)}{N}, \qquad \alpha_2 = \frac{\beta_2(U + \varepsilon I)}{N}, \qquad N = S_1 + S_2 + U + I + H + R,$$

and the controls $0 \leq u_i(t) \leq 1$ $(i = 1, 2, 3)$.

For equilibrium computations, we treat u_1, u_2, u_3 as constants (or as fixed mean levels), which is standard practice in threshold and steady-state analysis.

4.1. Disease-free equilibrium

The disease-free equilibrium corresponds to the absence of infection:

$$U = I = H = R = 0 \quad \Longrightarrow \quad \alpha_1 = \alpha_2 = 0.$$

Hence, the susceptible subsystem at equilibrium becomes

$$\begin{aligned} 0 &= A - \beta_1 u_1 S_1 + \beta_2(1 - u_1) S_2 - \delta S_1, \\ 0 &= \beta_1 u_1 S_1 - \beta_2(1 - u_1) S_2 - \delta S_2. \end{aligned} \tag{4.1}$$

Moreover, from the total population equation at DFE,

$$\frac{dN}{dt} = A - \delta N \quad \Rightarrow \quad N^0 = \frac{A}{\delta}.$$

Solving (4.1), we obtain the relation

$$\beta_1 u_1 S_1^0 = (\beta_2(1-u_1)+\delta)S_2^0,$$

using $S_1^0 + S_2^0 = N^0 = A/\delta$, we get the explicit DFE:

$$\mathcal{E}_0 = (S_1^0, S_2^0, 0, 0, 0, 0), \tag{4.2}$$

with

$$S_1^0 = \frac{\frac{A}{\delta}(\beta_2(1-u_1)+\delta)}{\beta_2(1-u_1)+\delta+\beta_1 u_1}, \qquad S_2^0 = \frac{\frac{A}{\delta}(\beta_1 u_1)}{\beta_2(1-u_1)+\delta+\beta_1 u_1}. \tag{4.3}$$

4.2. Endemic equilibrium

An endemic equilibrium $\mathcal{E}^* = (S_1^*, S_2^*, U^*, I^*, H^*, R^*)$ satisfies

$$U^* > 0 \quad \text{(and consequently } I^*, H^* \geq 0).$$

Define the composite removal rates

$$k_U = \tau_1 u_2 + \xi_1 + \delta, \qquad k_I = \gamma_1 + \eta_1 + \xi_1 + \delta, \qquad k_H = \tau_2 u_3 + \eta_2 + \delta.$$

From the steady-state equations of the infected subsystem, we obtain sequentially:

$$0 = \tau_1 u_2 U^* - k_I I^* \quad \Longrightarrow \quad I^* = \frac{\tau_1 u_2}{k_I} U^* \equiv q\, U^*, \qquad q := \frac{\tau_1 u_2}{k_I}, \tag{4.4}$$

$$0 = \gamma_1 I^* - k_H H^* \quad \Longrightarrow \quad H^* = \frac{\gamma_1}{k_H} I^* = \frac{\gamma_1 q}{k_H} U^*, \tag{4.5}$$

and from the recovered equation,

$$0 = \xi_1(U^* + I^*) + \tau_2 u_3 H^* - \delta R^* \quad \Longrightarrow \quad R^* = \frac{1}{\delta}\left[\xi_1(1+q) + \tau_2 u_3\left(\frac{\gamma_1 q}{k_H}\right)\right] U^*. \tag{4.6}$$

Next, introduce the endemic infection pressure

$$\lambda^* := \frac{U^* + \varepsilon I^*}{N^*} = \frac{(1+\varepsilon q)U^*}{N^*}, \qquad \alpha_1^* = \beta_1 \lambda^*, \quad \alpha_2^* = \beta_2 \lambda^*. \tag{4.7}$$

At equilibrium, the two susceptible equations form a linear system:

$$\begin{aligned} (\alpha_1^* + \beta_1 u_1 + \delta) S_1^* - \beta_2(1-u_1) S_2^* &= A, \\ -\beta_1 u_1 S_1^* + (\alpha_2^* + \beta_2(1-u_1) + \delta) S_2^* &= 0. \end{aligned} \tag{4.8}$$

Let the determinant be

$$\Delta(\lambda^*) = (\beta_1 \lambda^* + \beta_1 u_1 + \delta)\,(\beta_2 \lambda^* + \beta_2(1-u_1) + \delta) - \beta_1 u_1 \beta_2 (1-u_1). \tag{4.9}$$

Solving (4.8) yields

$$S_1^* = \frac{A(\beta_2 \lambda^* + \beta_2(1-u_1) + \delta)}{\Delta(\lambda^*)}, \qquad S_2^* = \frac{A(\beta_1 u_1)}{\Delta(\lambda^*)}. \tag{4.10}$$

Therefore, the EE can be written in closed form as

$$\mathcal{E}^* = \left(S_1^*,\, S_2^*,\, U^*,\, qU^*,\, \frac{\gamma_1 q}{k_H}U^*,\, \frac{1}{\delta}\left[\xi_1(1+q) + \tau_2 u_3\left(\frac{\gamma_1 q}{k_H}\right)\right]U^*\right), \tag{4.11}$$

where S_1^*, S_2^* depends on λ^* through (4.10) and λ^* is related to U^* through (4.7).

For the EE analysis, we treat controls u_1, u_2, u_3 as fixed constants in the interval $[0, 1]$ (or as fixed mean control levels), which is standard for equilibrium and threshold analysis. Define the composite removal rates

$$k_U = \tau_1 u_2 + \xi_1 + \delta, \qquad k_I = \gamma_1 + \eta_1 + \xi_1 + \delta, \qquad k_H = \tau_2 u_3 + \eta_2 + \delta,$$

and

$$q := \frac{\tau_1 u_2}{k_I}, \qquad \theta := 1 + \varepsilon q.$$

Recall from (4.4)–(4.6) that at equilibrium,

$$I^* = qU^*, \qquad H^* = \frac{\gamma_1 q}{k_H}U^*, \qquad R^* = \frac{1}{\delta}\left[\xi_1(1+q) + \tau_2 u_3\left(\frac{\gamma_1 q}{k_H}\right)\right]U^*.$$

Hence, the total population at the EE can be written as

$$N^* = S_1^* + S_2^* + c\,U^*, \tag{4.12}$$

where the constant $c > 0$ is given by

$$c := 1 + q + \frac{\gamma_1 q}{k_H} + \frac{1}{\delta}\left[\xi_1(1+q) + \tau_2 u_3\left(\frac{\gamma_1 q}{k_H}\right)\right]. \tag{4.13}$$

Define the endemic infection pressure

$$\lambda^* := \frac{U^* + \varepsilon I^*}{N^*} = \frac{\theta U^*}{N^*}.$$

By, using (4.12), we obtain the following:

$$U^* = \frac{\lambda^*}{\theta}N^* = \frac{\lambda^*}{\theta}\left(S_1^* + S_2^* + cU^*\right) \quad \Longrightarrow \quad U^* = \frac{\lambda^*\left(S_1^* + S_2^*\right)}{\theta - c\lambda^*}, \tag{4.14}$$

which requires

$$0 < \lambda^* < \frac{\theta}{c}. \tag{4.15}$$

Scalar endemicity equation. At equilibrium, the U-equation gives

$$0 = \alpha_1^* S_1^* + \alpha_2^* S_2^* - k_U U^*, \qquad \alpha_1^* = \beta_1\lambda^*,\ \alpha_2^* = \beta_2\lambda^*,$$

hence

$$\lambda^*\left(\beta_1 S_1^* + \beta_2 S_2^*\right) = k_U U^*. \tag{4.16}$$

Substituting (4.14) into (4.16) and canceling $\lambda^* > 0$, we obtain the *scalar endemicity equation*

$$G(\lambda) := (\beta_1 S_1(\lambda) + \beta_2 S_2(\lambda))(\theta - c\lambda) - k_U (S_1(\lambda) + S_2(\lambda)) = 0, \qquad 0 < \lambda < \frac{\theta}{c}, \tag{4.17}$$

where $S_1(\lambda), S_2(\lambda)$ are the unique positive solutions of the linear susceptible subsystem (4.8) after substituting

$$\alpha_1 = \beta_1 \lambda, \qquad \alpha_2 = \beta_2 \lambda.$$

Explicitly, using (4.9) and (4.10):

$$\Delta(\lambda) = (\beta_1\lambda + \beta_1 u_1 + \delta)(\beta_2\lambda + \beta_2(1-u_1) + \delta) - \beta_1 u_1 \beta_2 (1-u_1), \tag{4.18}$$

$$S_1(\lambda) = \frac{A(\beta_2\lambda + \beta_2(1-u_1) + \delta)}{\Delta(\lambda)}, \qquad S_2(\lambda) = \frac{A(\beta_1 u_1)}{\Delta(\lambda)}. \tag{4.19}$$

Theorem 3. *Assume all parameters are positive and that the controls satisfy* $0 \le u_i \le 1$. *If* $\mathcal{R}_0 > 1$, *then the system* (2.1) *admits at least one EE* $\mathcal{E}^* \in \Omega$. *If* $\mathcal{R}_0 \le 1$, *there is no EE in the interior of the feasible region.*

Proof. The next-generation threshold result implies that $\mathcal{R}_0 > 1$ is necessary for the persistence of infection and instability of the DFE. while $\mathcal{R}_0 \le 1$ implies the local attraction of the DFE. Moreover, an EE corresponds to a solution $\lambda^* \in (0, \theta/c)$ of (4.17). At $\lambda \to 0^+$, we have $S_1(\lambda) \to S_1^0$ and $S_2(\lambda) \to S_2^0$ (DFE values), thus

$$G(0^+) = (\beta_1 S_1^0 + \beta_2 S_2^0)\theta - k_U(S_1^0 + S_2^0).$$

Using $S_1^0 + S_2^0 = N^0 = A/\delta$ and the standard construction of $\mathcal{R}_0$ for this class of models, $G(0^+)$ has the same sign as $(\mathcal{R}_0 - 1)$. Hence $G(0^+) > 0$ when $\mathcal{R}_0 > 1$. On the other hand, as $\lambda \to (\theta/c)^-$, the factor $(\theta - c\lambda) \to 0^+$ while $S_1(\lambda) + S_2(\lambda)$ remains nonnegative, resulting in $G(\lambda) < 0$ sufficiently close to θ/c. By the continuity of G, there exists $\lambda^* \in (0, \theta/c)$ such that $G(\lambda^*) = 0$, establishing the existence of an EE when $\mathcal{R}_0 > 1$. When $\mathcal{R}_0 \le 1$, $G(0^+) \le 0$ and no positive root occurs in $(0, \theta/c)$. □

Indeed, according to Theorem 3, every value of $R_0 > 1$ entails at least one EE and only establishes it. In the absence of supplementary conditions placed on it, uniqueness regarding a typical monoculture endemic function $G(\lambda)$ is not posited. The EE is unique if $G(\lambda)$ is monotonic and decreasing within $(0, \frac{0}{\theta})$. It was not analytically demonstrated in this study that such monotonicity holds for all λ values allowed by the parameter values, a point masked only by numerical verification against the primary parameter sets used in this study.

Remark 1. *In many epidemiological settings,* $S_1(\lambda)$ *and* $S_2(\lambda)$ *decrease in* λ *on* $(0, \theta/c)$, *which makes* $G(\lambda)$ *strictly decrease. In that case,* (4.17) *admits a* unique *root* λ^* *and consequently the EE* $\mathcal{E}^*$ *is unique. This monotonicity can be verified numerically for fitted parameter sets (and typically holds for positive parameters and* $0 < u_1 < 1$*).*

The dependencies of endemic infective and basic reproduction number on the transmission level and testing control are displayed in Figure 1. This illustrates how increased testing efforts can bring down the total infective burden by pushing the system closer to the elimination threshold.

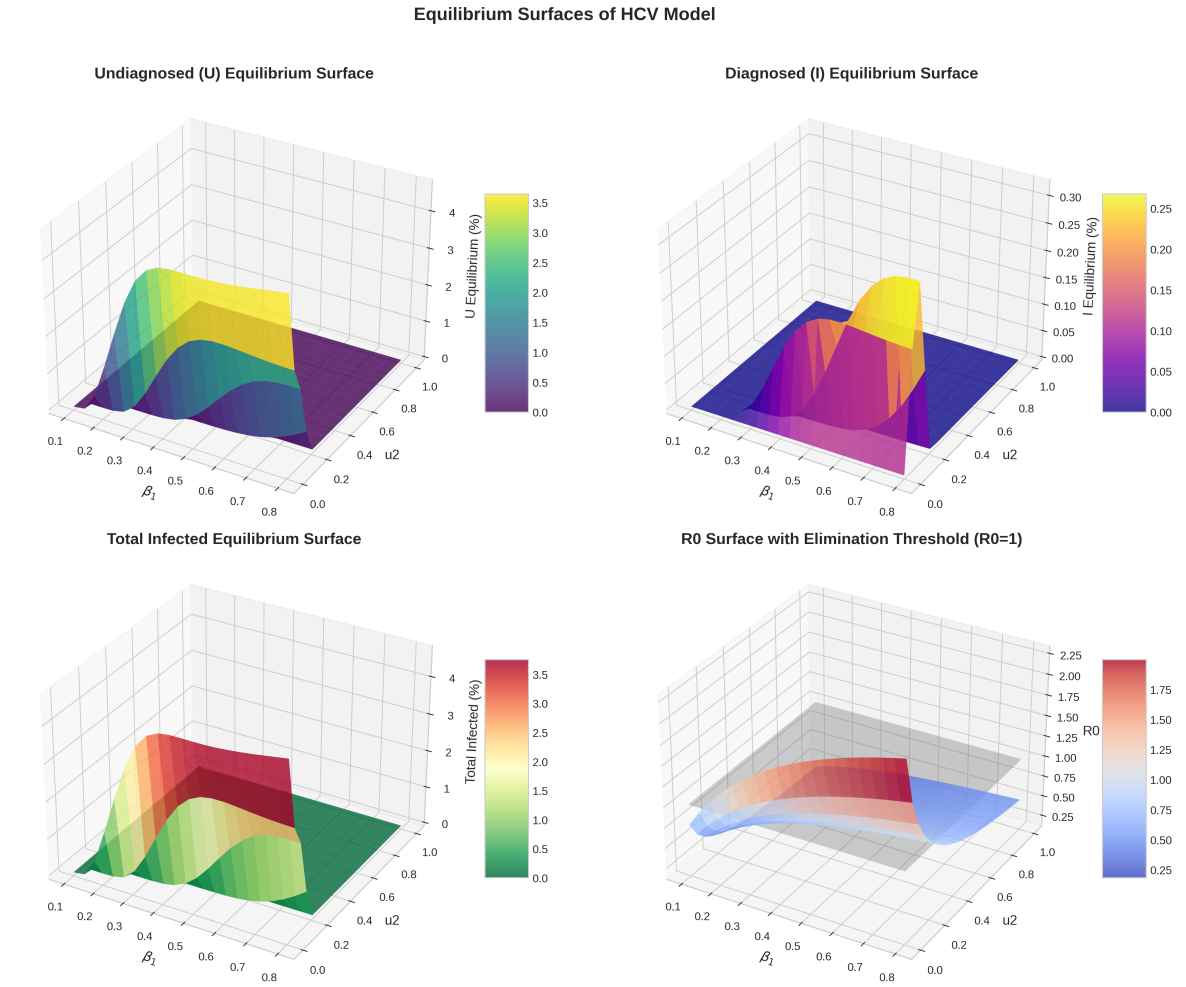

Figure 1. Equilibrium surfaces of the HCV model under varying transmission and control. The 3D surfaces illustrate the steady-state prevalence and reproductive dynamics as functions of the transmission rate (β_1) and the testing control (u_2). **(Top Left)** Undiagnosed (U) equilibrium surface: This shows the percentage of the population in the undiagnosed infected state, peaking at low control and high transmission. **(Top right)** Diagnosed (I) equilibrium surface: represents the infected population that has been identified; the surface shows a distinct peak where testing control is high enough to move individuals from U to I, but transmission remains active. **(Bottom left)** Total infected equilibrium surface: The aggregate prevalence ($U + I$), indicating the overall disease burden across the parameter space. **(Bottom right)** R_0 surface with elimination threshold: The basic reproduction number surface intersected by a semi-transparent grey plane at $R_0 = 1$. The region where the surface lies below this plane represents the parameter combinations necessary for disease elimination.

5. Basic reproduction number $\mathcal{R}_0$

We derive the basic reproduction number $\mathcal{R}_0$ for system (2.1) using the next-generation matrix method of van den Driessche and Watmough [18]. The infection process in the model is driven by the

undiagnosed infected class U and the diagnosed infected class I through the incidence terms

$$\alpha_1 = \frac{\beta_1(U + \varepsilon I)}{N}, \qquad \alpha_2 = \frac{\beta_2(U + \varepsilon I)}{N},$$

where $\varepsilon \in (0, 1]$ modifies the relative infectiousness of the diagnosed class I (e.g., due to behavioral changes, reduced contact rate or partial isolation).

In a DFE, $U = I = H = R = 0$ and $N^0 = A/\delta$. The susceptible components are

$$S_1^0 = \frac{\frac{A}{\delta}(\beta_2(1 - u_1) + \delta)}{\beta_2(1 - u_1) + \delta + \beta_1 u_1}, \qquad S_2^0 = \frac{\frac{A}{\delta}(\beta_1 u_1)}{\beta_2(1 - u_1) + \delta + \beta_1 u_1}. \tag{5.1}$$

Define the *effective transmission weight* of DFE

$$k := \frac{\beta_1 S_1^0 + \beta_2 S_2^0}{N^0}, \qquad N^0 = \frac{A}{\delta}. \tag{5.2}$$

Then the total rate of production of *new infections* in U at early invasion is

$$\mathcal{F}_U = k\,(U + \varepsilon I).$$

We take the vector infected state to be

$$x = (U, I, H)^\top.$$

Although H does not directly generate new infections in the given incidence term, it is included to maintain the closed status of the infected block during transitions.

Introduce the (positive) transition-rate aggregates:

$$k_U = \tau_1 u_2 + \xi_1 + \delta, \qquad k_I = \gamma_1 + \eta_1 + \xi_1 + \delta, \qquad k_H = \tau_2 u_3 + \eta_2 + \delta. \tag{5.3}$$

Write the infected subsystem in the standard form

$$\dot{x} = \mathcal{F}(x) - \mathcal{V}(x),$$

where $\mathcal{F}$ collects new infection terms and $\mathcal{V}$ collects all other transfers.

New infection terms. Only U receives new infections, and hence in the DFE,

$$\mathcal{F}(x) = \begin{pmatrix} k\,(U + \varepsilon I) \\ 0 \\ 0 \end{pmatrix}.$$

Therefore, the Jacobian matrix $F = \left[\frac{\partial \mathcal{F}_i}{\partial x_j}\right]_{\mathcal{E}_0}$ is

$$F = \begin{pmatrix} k & k\varepsilon & 0 \\ 0 & 0 & 0 \\ 0 & 0 & 0 \end{pmatrix}. \tag{5.4}$$

Transition terms. From the model equations,

$$\frac{dU}{dt} = \underbrace{k(U + \varepsilon I)}_{\mathcal{F}_U} - k_U U, \qquad \frac{dI}{dt} = \tau_1 u_2 U - k_I I, \qquad \frac{dH}{dt} = \gamma_1 I - k_H H.$$

Hence, taking $\mathcal{V}$ as "outflow minus inflow" (excluding new infections),

$$\mathcal{V}(x) = \begin{pmatrix} k_U U \\ k_I I - \tau_1 u_2 U \\ k_H H - \gamma_1 I \end{pmatrix},$$

and the Jacobian matrix $V = \left[\frac{\partial \mathcal{V}_i}{\partial x_j}\right]_{\mathcal{E}_0}$ is

$$V = \begin{pmatrix} k_U & 0 & 0 \\ -\tau_1 u_2 & k_I & 0 \\ 0 & -\gamma_1 & k_H \end{pmatrix}. \tag{5.5}$$

Since $k_U, k_I, k_H > 0$, the matrix V is nonsingular and V^{-1} exists.

The next-generation matrix is $K = FV^{-1}$ and

$$\mathcal{R}_0 = \rho(K),$$

where $\rho(\cdot)$ denotes the spectral radius.

Because F has only its first row nonzero, K has rank one and only one possible nonzero eigenvalue, equal to the entry $(1, 1)$ of FV^{-1} (after simplification). Instead of explicitly computing the full inverse, we compute the expected infectious contribution along the infection pathway $U \to I \to H$.

Pathwise interpretation (equivalent to FV^{-1}). A newly infected individual enters U and produces new infections at a rate k while in U, with a mean duration $1/k_U$. Thus, the expected number of secondary cases generated during the U stage is

$$k \cdot \frac{1}{k_U}.$$

Individuals leave U to I at a rate $\tau_1 u_2$, so the probability of progressing from U to I before leaving by recovery/death is

$$\mathbb{P}(U \to I) = \frac{\tau_1 u_2}{k_U}.$$

Once in I, individuals generate new infections at a reduced rate $k\varepsilon$, and remain in I for a mean duration $1/k_I$. Hence, the expected number of secondary cases generated during the I stage is

$$\left(\frac{\tau_1 u_2}{k_U}\right) \cdot (k\varepsilon) \cdot \frac{1}{k_I} = k \cdot \frac{\varepsilon \tau_1 u_2}{k_U k_I}.$$

The hospitalized class H does not appear in the incidence term $k(U + \varepsilon I)$ and therefore does not contribute to the generation of new infections in the present formulation.

Adding both contributions yields

$$\mathcal{R}_0 = k\left(\frac{1}{k_U} + \frac{\varepsilon\tau_1 u_2}{k_U k_I}\right) = \frac{k}{k_U}\left(1 + \frac{\varepsilon\tau_1 u_2}{k_I}\right), \tag{5.6}$$

where k is given in (5.2) and k_U, k_I in (5.3). Equivalently, substituting k explicitly,

$$\mathcal{R}_0 = \frac{\beta_1 S_1^0 + \beta_2 S_2^0}{N^0}\,\frac{1}{\tau_1 u_2 + \xi_1 + \delta}\left(1 + \frac{\varepsilon\tau_1 u_2}{\gamma_1 + \eta_1 + \xi_1 + \delta}\right), \tag{5.7}$$

with S_1^0, S_2^0, N^0 given by (5.1).

The expression (5.7) decomposes $\mathcal{R}_0$ into

- A *contact/transmission factor* $\frac{\beta_1 S_1^0 + \beta_2 S_2^0}{N^0}$, which is indirectly reduced by media awareness u_1 by shifting the mass from S_1 to S_2 and altering the weighted risk;
- An *average infectious time in the undiagnosed class* $\frac{1}{\tau_1 u_2 + \xi_1 + \delta}$, which decreases as the intensity of the test u_2 increases;
- An *additional contribution to the diagnosed-stage* $\left(1 + \frac{\varepsilon\tau_1 u_2}{k_I}\right)$, capturing that a fraction of U progresses to I and remains infectious (scaled by ε) for the mean time $1/k_I$.

Therefore, increasing u_2 reduces the undiagnosed infectious period (which tends to decrease $\mathcal{R}_0$), while the contribution of the diagnosed stage is moderated by ε and the removal parameters in k_I (hospitalization, recovery, and mortality). Treatment control u_3 does not enter $\mathcal{R}_0$ in this formulation because treatment acts in H and H is not modeled as a source of new infection; however, u_3 strongly affects prevalence and burden by reducing the time in H and increasing recovery.

6. Stability analysis

6.1. Local stability of the DFE

Let $\mathcal{E}_0 = (S_1^0, S_2^0, 0, 0, 0, 0)$ be the DFE given in (4.2) and (4.3). We analyze its local stability using the Jacobian matrix of the system (2.1).

Denote the state vector by

$$X = (S_1, S_2, U, I, H, R)^\top,$$

and let $J(X)$ be the Jacobian matrix. In DFE, the system admits a natural decomposition into (i) the *uninfected* variables (S_1, S_2, R) and (ii) the *infected* variables (U, I, H). In particular, the linearized dynamics near $\mathcal{E}_0$ has the upper-triangular form of the block.

$$J(\mathcal{E}_0) = \begin{pmatrix} J_{SS} & J_{SI} \\ 0 & J_{II} \end{pmatrix}.$$

Therefore, the eigenvalues of $J(\mathcal{E}_0)$ are the union of the eigenvalues of J_{SS} and J_{II}.

The infected block is obtained from the linearization of the infected subsystem:

$$\frac{dU}{dt} = k(U + \varepsilon I) - k_U U, \qquad \frac{dI}{dt} = \tau_1 u_2 U - k_I I, \qquad \frac{dH}{dt} = \gamma_1 I - k_H H,$$

where

$$k = \frac{\beta_1 S_1^0 + \beta_2 S_2^0}{N^0}, \quad N^0 = \frac{A}{\delta}, \quad k_U = \tau_1 u_2 + \xi_1 + \delta, \quad k_I = \gamma_1 + \eta_1 + \xi_1 + \delta, \quad k_H = \tau_2 u_3 + \eta_2 + \delta.$$

Hence

$$J_{II} = \begin{pmatrix} k - k_U & k\varepsilon & 0 \\ \tau_1 u_2 & -k_I & 0 \\ 0 & \gamma_1 & -k_H \end{pmatrix}.$$

Since $-k_H < 0$, one eigenvalue is always $-k_H$. The remaining two eigenvalues are those of the 2×2 block

$$M = \begin{pmatrix} k - k_U & k\varepsilon \\ \tau_1 u_2 & -k_I \end{pmatrix}.$$

The trace and determinant of M are

$$\mathrm{tr}(M) = k - (k_U + k_I), \qquad \det(M) = -(k - k_U)k_I - k\varepsilon\tau_1 u_2.$$

Using the next-generation matrix derivation, the basic reproduction number is

$$\mathcal{R}_0 = \frac{k}{k_U}\left(1 + \frac{\varepsilon\,\tau_1 u_2}{k_I}\right). \tag{6.1}$$

Theorem 4. *The DFE $\mathcal{E}_0$ is locally asymptotically stable if $\mathcal{R}_0 < 1$ and unstable if $\mathcal{R}_0 > 1$.*

Proof. By the next-generation theorem, $\mathcal{R}_0 = \rho(FV^{-1})$ and the infected subsystem has all eigenvalues with negative real parts if and only if $\mathcal{R}_0 < 1$. Because $J(\mathcal{E}_0)$ is the upper-triangular block and the uninfected block J_{SS} has a negative diagonal-dominant structure under positive parameters, the sign of the dominant eigenvalue is determined by J_{II}. Thus, $\mathcal{E}_0$ is locally asymptotically stable for $\mathcal{R}_0 < 1$ and unstable for $\mathcal{R}_0 > 1$. □

6.2. Global stability of the DFE

The localized threshold outcomes in Theorem 4 consider the local asymptotic stability of the DFE with $\mathcal{R}_0 < 1$. Obtaining global asymptotic stability results for the full model becomes tricky, as the nonlinear incidence term is time-dependent and depends specifically on the number of susceptible elements and the total population. Since fully agreeing with the statement of a disease-free, stable whole with the aforementioned system would be invalidated, we do not claim a completely global disease-free stable outcome for the unrestricted system in this article.

Theorem 5. *If $\mathcal{R}_0 \leq 1$, the disease-free equilibrium $\mathcal{E}_0$ is locally stabilized asymptotically. Additionally, in the parameter set considered in the numerical experiments, all trajectories with initial data in a feasible region tend to the disease-free state, which validates the action of keeping the disease below the threshold to eliminate the disease.*

6.3. Local stability of the EE

Assume $\mathcal{R}_0 > 1$ so that an EE $\mathcal{E}^*$ exists (Section 3). We outline a practical and rigorous local stability test based on the characteristic polynomial of the Jacobian evaluated at $\mathcal{E}^*$.

Let $J^* = J(\mathcal{E}^*)$. Because the recovered class does not feed back into infection (except via the total population N in incidence terms), the dominant stability behavior is governed by the infected block. Let the vector of the infected-state be $x = (U, I, H)^\top$. Write the infected subsystem near $\mathcal{E}^*$ in linear form:

$$\dot{x} = A^* x + \text{higher-order terms},$$

where A^* is the Jacobian submatrix 3×3 with respect to (U, I, H) at $\mathcal{E}^*$:

$$A^* = \begin{pmatrix} \partial_U f_U & \partial_I f_U & 0 \\ \tau_1 u_2 & -k_I & 0 \\ 0 & \gamma_1 & -k_H \end{pmatrix}_{\mathcal{E}^*}.$$

Here $f_U = \alpha_1 S_1 + \alpha_2 S_2 - k_U U$ and the derivatives $\partial_U f_U, \partial_I f_U$ account for the dependence of (α_1, α_2) on (U, I) and on N on $\mathcal{E}^*$.

Let the characteristic polynomial of A^* be

$$\chi(\lambda) = \lambda^3 + a_1\lambda^2 + a_2\lambda + a_3. \tag{6.2}$$

A direct computation gives the coefficients in terms of trace and principal minors:

$$a_1 = -\text{tr}(A^*) = k_H + k_I - \partial_U f_U, \tag{6.3}$$

$$a_2 = \text{sum of principal } 2 \times 2 \text{ minors of } A^*, \tag{6.4}$$

$$a_3 = -\det(A^*). \tag{6.5}$$

Explicitly, using the structure of A^*:

$$a_2 = (k_I k_H) - (\partial_U f_U)(k_I + k_H) - \tau_1 u_2\, \partial_I f_U, \tag{6.6}$$

$$a_3 = -\left[(\partial_U f_U)(k_I k_H) + (\tau_1 u_2)(\partial_I f_U) k_H\right]. \tag{6.7}$$

Theorem 6 (Conditional Routh-Hurwitz criterion for local stability of $\mathcal{E}^*$)**.** *The endemic equilibrium $\mathcal{E}^*$ is locally asymptotically stable if the Routh-Hurwitz conditions hold:*

$$a_1 > 0, \qquad a_2 > 0, \qquad a_3 > 0, \qquad a_1 a_2 > a_3,$$

where a_1, a_2, a_3 are given by (6.3)–(6.7)*.*

Consequently, the local asymptotic stability of an endemic equilibrium is conditional on the verification of the Routh-Hurwitz inequalities for the equilibrium under consideration; it is not claimed here for all parameter regimes with $\mathcal{R}_0 > 1$.

Theorem 6 provides a local stability criterion for an EE under a condition. It does not claim that the coefficient sign conditions $a_1, a_2, a_3 > 0$, and $a_1 a_2 > a_3$ are automatically valid for all admissible parameter regimes with $\mathcal{R}_0 > 1$. Instead, these inequalities depend on the specific EE and model parameters, and in the present study, they are numerically verified for representative parameter sets.

Remark 2. *For a set of estimated parameters, compute $\mathcal{E}^*$ using the hybrid Newton bisection scheme (previous subsection), then evaluate $\partial_U f_U$ and $\partial_I f_U$ numerically (finite differences in f_U in $\mathcal{E}^*$ are sufficient), compute a_1, a_2, a_3 and verify inequalities. This provides a stable/unstable classification of $\mathcal{E}^*$ without requiring closed-form eigenvalues.*

6.4. Global stability of the EE

In this subsection, we establish the global asymptotic stability (GAS) of the EE under additional biologically interpretable conditions. Throughout, we assume that the controls u_1, u_2, and u_3 are constant in the interval $[0, 1]$.

6.4.1. Additional assumptions for global analysis

(A1) **No disease-induced mortality:** $\eta_1 = \eta_2 = 0$. (This yields an asymptotically constant total population.)

(A2) **Unique endemic equilibrium:** for $\mathcal{R}_0 > 1$ the scalar endemicity equation admits a unique root λ^* (see Remark 1), and hence the EE $\mathcal{E}^*$ is unique.

(A3) **All parameters are strictly positive** and the solutions remain in the feasible invariant set Ω.

6.4.2. Consequences of (A1)

With $\eta_1 = \eta_2 = 0$, summing the model equations gives the following result:

$$\frac{dN}{dt} = A - \delta N,$$

hence

$$N(t) \to N^0 := \frac{A}{\delta} \quad \text{as } t \to \infty,$$

and the standard incidence terms become asymptotically equivalent to

$$\alpha_1 = \frac{\beta_1(U + \varepsilon I)}{N^0}, \qquad \alpha_2 = \frac{\beta_2(U + \varepsilon I)}{N^0}.$$

Therefore, long-term dynamics are governed by an asymptotically autonomous system with a constant population N^0.

For notational convenience, define the constants (with $\eta_1 = \eta_2 = 0$)

$$k_U = \tau_1 u_2 + \xi_1 + \delta, \qquad k_I = \gamma_1 + \xi_1 + \delta, \qquad k_H = \tau_2 u_3 + \delta.$$

Let the unique EE for $\mathcal{R}_0 > 1$ be

$$\mathcal{E}^* = (S_1^*, S_2^*, U^*, I^*, H^*, R^*), \qquad U^*, I^*, H^* > 0.$$

6.4.3. Lyapunov function

Consider the Volterra-type Lyapunov function

$$\begin{aligned} \mathcal{V}(t) = &\left(S_1 - S_1^* - S_1^* \ln \frac{S_1}{S_1^*}\right) + \left(S_2 - S_2^* - S_2^* \ln \frac{S_2}{S_2^*}\right) \\ &+ \left(U - U^* - U^* \ln \frac{U}{U^*}\right) + c_1 \left(I - I^* - I^* \ln \frac{I}{I^*}\right) + c_2 \left(H - H^* - H^* \ln \frac{H}{H^*}\right), \end{aligned} \tag{6.8}$$

where the positive weights are chosen as

$$c_1 := \frac{\varepsilon k_I}{\tau_1 u_2}, \qquad c_2 := \frac{\varepsilon k_H}{\gamma_1} c_1 = \frac{\varepsilon k_I k_H}{\tau_1 u_2 \gamma_1}. \tag{6.9}$$

Clearly, $\mathcal{V} \geq 0$ for all positive states and $\mathcal{V} = 0$ if and only if $(S_1, S_2, U, I, H) = (S_1^*, S_2^*, U^*, I^*, H^*)$.

6.4.4. Derivative of $\mathcal{V}$ along solutions

Using $\frac{d}{dt}\left(x - x^* - x^* \ln \frac{x}{x^*}\right) = \left(1 - \frac{x^*}{x}\right)\dot{x}$, we obtain

$$\dot{\mathcal{V}} = \left(1 - \frac{S_1^*}{S_1}\right)\dot{S}_1 + \left(1 - \frac{S_2^*}{S_2}\right)\dot{S}_2 + \left(1 - \frac{U^*}{U}\right)\dot{U} + c_1\left(1 - \frac{I^*}{I}\right)\dot{I} + c_2\left(1 - \frac{H^*}{H}\right)\dot{H}. \tag{6.10}$$

We introduce the (constant population) incidence term

$$\Lambda := \frac{U + \varepsilon I}{N^0}, \qquad \text{so that} \qquad \alpha_1 S_1 + \alpha_2 S_2 = (\beta_1 S_1 + \beta_2 S_2)\Lambda.$$

At equilibrium, define

$$\Lambda^* := \frac{U^* + \varepsilon I^*}{N^0}.$$

From the U-equilibrium equation,

$$(\beta_1 S_1^* + \beta_2 S_2^*)\Lambda^* = k_U U^*. \tag{6.11}$$

Also, from the equations of the I- and H-equilibrium,

$$\tau_1 u_2 U^* = k_I I^*, \qquad \gamma_1 I^* = k_H H^*. \tag{6.12}$$

Key inequality. We repeatedly use the standard inequality for $z > 0$:

$$1 - z + \ln z \le 0, \quad \text{with equality iff } z = 1,$$

and the arithmetic mean and geometric mean inequality.

6.4.5. Main estimate

After substituting the system's equations (with $\eta_1 = \eta_2 = 0$) into (6.10), regrouping the terms using the equilibrium identities (6.11) and (6.12), and applying AM-GM, one obtains the bound

$$\begin{aligned}\dot{\mathcal{V}} \le &-\delta\,(S_1 - S_1^*)^2\,\frac{1}{S_1} - \delta\,(S_2 - S_2^*)^2\,\frac{1}{S_2} - k_U U^*\left(1 - \frac{U}{U^*} + \ln\frac{U}{U^*}\right)\\ &-\varepsilon k_I I^*\left(1 - \frac{I}{I^*} + \ln\frac{I}{I^*}\right) - \varepsilon k_H H^*\left(1 - \frac{H}{H^*} + \ln\frac{H}{H^*}\right).\end{aligned} \tag{6.13}$$

Each term on the right-hand side is non-positive, hence $\dot{\mathcal{V}} \le 0$.

Moreover, $\dot{\mathcal{V}} = 0$ holds only when

$$S_1 = S_1^*, \quad S_2 = S_2^*, \quad U = U^*, \quad I = I^*, \quad H = H^*.$$

Theorem 7. *Assume (A1)–(A3). If $\mathcal{R}_0 > 1$, then the unique EE $\mathcal{E}^*$ is globally asymptotically stable in the interior of the feasible region Ω.*

Proof. From (6.8), $\mathcal{V}$ is positive definite with a global minimum at $\mathcal{E}^*$. By (6.13), $\dot{\mathcal{V}} \leq 0$ along trajectories. Let

$$\mathcal{M} = \left\{X \in \Omega : \dot{\mathcal{V}}(X) = 0\right\}.$$

By the characterization above, the largest invariant subset of $\mathcal{M}$ is the singleton $\{\mathcal{E}^*\}$. Therefore, by LaSalle's invariance principle, every solution with positive initial data converges to $\mathcal{E}^*$. This proves global asymptotic stability. □

Remark 3. *Assumption (A1) assumes that the population is asymptotically constant, which is common in HCV transmission when disease-induced deaths are negligible compared to natural turnover on the time horizon of interest. If $\eta_1, \eta_2 > 0$ are retained, a global EE Lyapunov proof is still possible but requires a more technical construction to handle the variable denominator $N(t)$ in the standard incidence.*

A comprehensive stability summary in the baseline regime is presented in Figure 2.

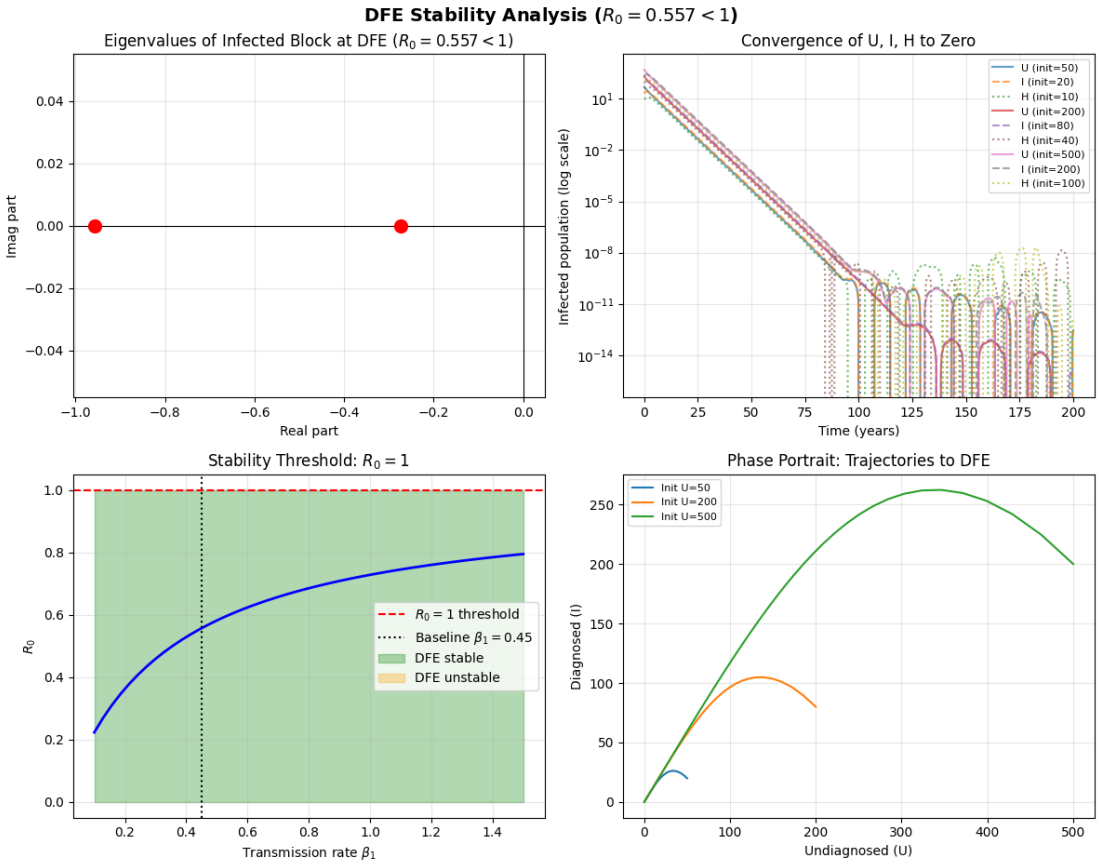

Figure 2. Stability analysis of the DFE for $\mathcal{R}_0 < 1$. **(Top left)** Eigenvalues of the infected Jacobian (all $\mathrm{Re}(\lambda) < 0$). **(Top right)** Time series of $U(t), I(t), H(t)$ converging to zero (log scale). **(Bottom left)** $\mathcal{R}_0$ as a function of β_1 showing the stability threshold at $\mathcal{R}_0 = 1$. **(Bottom right)** Phase portrait in (U, I) with trajectories approaching the origin. The results confirm Theorems 4 and 5: the DFE is locally and globally asymptotically stable when $\mathcal{R}_0$<1.

In Figure 3, a demonstration of phase-plane trajectories is given, showing how various regimes of parameters bring about convergence towards the disease-free and endemic equilibria.

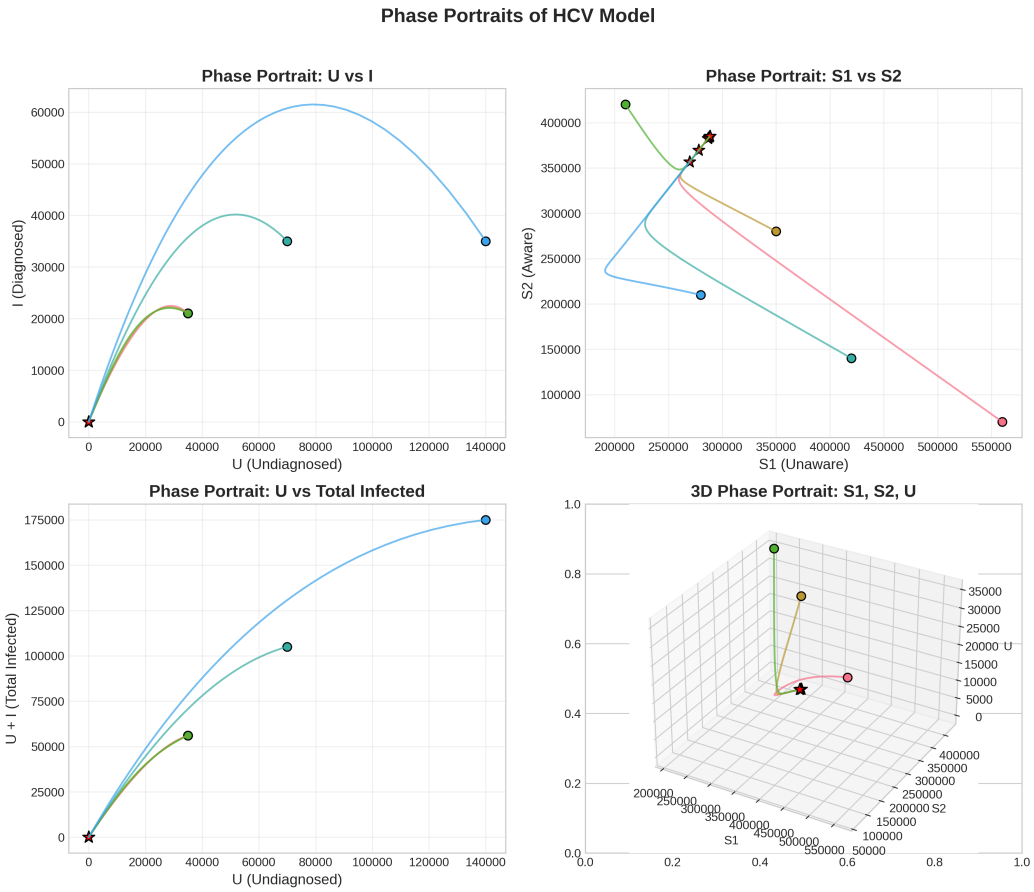

Figure 3. Phase-plane dynamics of infected compartments illustrating stability of the DFE and EE under different parameter regimes.

7. Sensitivity and PRCC analysis of $\mathcal{R}_0$

This section quantifies how uncertainty in model parameters and intervention levels influences the basic reproduction number $\mathcal{R}_0$. We perform (i) *local (normalized) sensitivity* analysis and (ii) *global sensitivity* analysis using PRCC with LHS.

7.1. Local sensitivity indices of $\mathcal{R}_0$

For a parameter p, the (normalized forward) sensitivity index of $\mathcal{R}_0$ is defined by

$$\Upsilon_p^{\mathcal{R}_0} = \frac{p}{\mathcal{R}_0}\frac{\partial \mathcal{R}_0}{\partial p} = \frac{\partial \ln(\mathcal{R}_0)}{\partial \ln(p)}. \tag{7.1}$$

A positive (negative) value indicates that increasing p increases (decreases) $\mathcal{R}_0$.

7.1.1. Closed-form local indices for key parameters

To present interpretable sensitivities, it is common to treat (S_1^0, S_2^0) as fixed at the baseline DFE (i.e., their dependence on u_1 is handled separately). Define

$$k_0 := \frac{\beta_1 S_1^0 + \beta_2 S_2^0}{N^0}, \quad D_U := \tau_1 u_2 + \xi_1 + \delta, \quad D_I := \gamma_1 + \eta_1 + \xi_1 + \delta, \quad \Phi := 1 + \frac{\varepsilon \tau_1 u_2}{D_I}.$$

Then $\mathcal{R}_0 = k_0 D_U^{-1} \Phi$.

Transmission parameters β_1, β_2. Since k_0 depends linearly on β_1, β_2,

$$\Upsilon_{\beta_1}^{\mathcal{R}_0} = \frac{\beta_1 S_1^0}{\beta_1 S_1^0 + \beta_2 S_2^0}, \qquad \Upsilon_{\beta_2}^{\mathcal{R}_0} = \frac{\beta_2 S_2^0}{\beta_1 S_1^0 + \beta_2 S_2^0}. \tag{7.2}$$

Hence $0 < \Upsilon_{\beta_1}^{\mathcal{R}_0} < 1$, $0 < \Upsilon_{\beta_2}^{\mathcal{R}_0} < 1$, and $\Upsilon_{\beta_1}^{\mathcal{R}_0} + \Upsilon_{\beta_2}^{\mathcal{R}_0} = 1$.

Testing pathway τ_1 and testing control u_2. Note that τ_1 and u_2 appear through D_U and Φ only through the product $\tau_1 u_2$. Let $x := \tau_1 u_2$. Then

$$\ln(\mathcal{R}_0) = \ln k_0 - \ln(x + \xi_1 + \delta) + \ln\Big(1 + \frac{\varepsilon x}{D_I}\Big).$$

A direct calculation gives

$$\frac{\partial \ln(\mathcal{R}_0)}{\partial x} = -\frac{1}{x + \xi_1 + \delta} + \frac{\varepsilon / D_I}{1 + \varepsilon x / D_I}. \tag{7.3}$$

Therefore,

$$\Upsilon_{\tau_1}^{\mathcal{R}_0} = \tau_1 u_2 \left[-\frac{1}{D_U} + \frac{\varepsilon}{D_I + \varepsilon \tau_1 u_2} \right], \qquad \Upsilon_{u_2}^{\mathcal{R}_0} = \tau_1 u_2 \left[-\frac{1}{D_U} + \frac{\varepsilon}{D_I + \varepsilon \tau_1 u_2} \right]. \tag{7.4}$$

Thus $\Upsilon_{\tau_1}^{\mathcal{R}_0} = \Upsilon_{u_2}^{\mathcal{R}_0}$ under this formulation.

Infectiousness modifier ε. Only Φ depends on ε, hence

$$\Upsilon_{\varepsilon}^{\mathcal{R}_0} = \frac{\varepsilon}{\Phi} \frac{\partial \Phi}{\partial \varepsilon} = \frac{\varepsilon \tau_1 u_2 / D_I}{1 + \varepsilon \tau_1 u_2 / D_I} = \frac{\varepsilon \tau_1 u_2}{D_I + \varepsilon \tau_1 u_2}. \tag{7.5}$$

Removal parameters ξ_1 and δ. The parameter ξ_1 appears in both D_U and D_I; δ appears in D_U and D_I and also in $N^0 = A/\delta$ and (S_1^0, S_2^0) (hence its full derivative includes additional terms). If we have k_0 fixed,

$$\Upsilon_{\xi_1}^{\mathcal{R}_0} = -\frac{\xi_1}{D_U} - \frac{\xi_1}{D_I} \cdot \frac{\varepsilon \tau_1 u_2 / D_I}{1 + \varepsilon \tau_1 u_2 / D_I} = -\frac{\xi_1}{D_U} - \frac{\xi_1 \, \varepsilon \tau_1 u_2}{D_I \, (D_I + \varepsilon \tau_1 u_2)}. \tag{7.6}$$

A similar expression holds for δ if k_0 is treated as fixed:

$$\Upsilon_{\delta}^{\mathcal{R}_0} = -\frac{\delta}{D_U} - \frac{\delta \, \varepsilon \tau_1 u_2}{D_I \, (D_I + \varepsilon \tau_1 u_2)} \quad \text{(holding } k_0 \text{ fixed)}. \tag{7.7}$$

In the complete model, δ also influences k_0 through $N^0 = A/\delta$ and S_1^0, S_2^0; thus, for numerical reporting, we compute $\Upsilon_{\delta}^{\mathcal{R}_0}$ by finite differences.

7.1.2. Local sensitivity of $\mathcal{R}_0$ with respect to awareness control u_1

Unlike u_2, awareness control u_1 affects $\mathcal{R}_0$ primarily through $k_0(u_1) = \frac{\beta_1 S_1^0(u_1) + \beta_2 S_2^0(u_1)}{N^0}$. Therefore,

$$\Upsilon_{u_1}^{\mathcal{R}_0} = \frac{u_1}{k_0(u_1)} \frac{dk_0(u_1)}{du_1}. \tag{7.8}$$

Because $k_0(u_1)$ is a smooth rational function, we compute $\Upsilon_{u_1}^{\mathcal{R}_0}$ numerically using a finite centered difference:

$$\Upsilon_{u_1}^{\mathcal{R}_0} \approx \frac{u_1}{\mathcal{R}_0(u_1)} \cdot \frac{\mathcal{R}_0(u_1 + h) - \mathcal{R}_0(u_1 - h)}{2h}, \quad h \ll 1.$$

7.1.3. Local sensitivity table

Table 3 reports the normalized local sensitivity indices of $\mathcal{R}_0$ with respect to key epidemiological parameters and control variables, evaluated in the set of baseline parameters. The results identify transmission parameters as the dominant positive contributors to $\mathcal{R}_0$, while diagnostic tests and awareness controls exhibit the strongest negative influence, indicating their effectiveness in reducing transmission potential.

The local sensitivity indices computed in the baseline parameter set are reported in Table 3 and visualized in Figure 4. Figure 4 provides a graphical representation of the local sensitivity indices listed in Table 3. The bar graph highlights the relative magnitude and direction of the influence of each parameter on $\mathcal{R}_0$, clearly illustrating the dominant role of transmission rates and the substantial mitigating effect of diagnostic testing and awareness interventions.

Table 3. Local sensitivity indices of $\mathcal{R}_0$ at the baseline parameter set ($\mathcal{R}_0 \approx 0.557$).

Parameter	$\Upsilon_p^{\mathcal{R}_0}$	**Effect on $\mathcal{R}_0$**
β_1	0.427	Increases $\mathcal{R}_0$
β_2	0.552	Increases $\mathcal{R}_0$
ε	0.279	Increases $\mathcal{R}_0$
τ_1	−0.506	Decreases $\mathcal{R}_0$
u_2	−0.506	Decreases $\mathcal{R}_0$
ξ_1	−0.250	Decreases $\mathcal{R}_0$
γ_1	−0.216	Decreases $\mathcal{R}_0$
η_1	−0.004	Weak decrease
δ	−0.003	Weak decrease
u_1	−0.318	Decreases $\mathcal{R}_0$

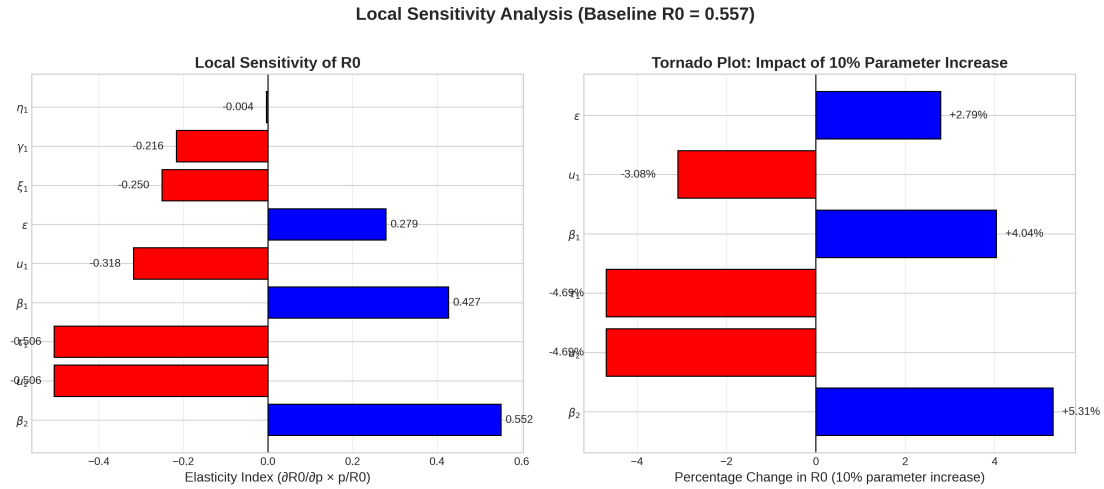

Figure 4. Local sensitivity indices of the basic reproduction number $\mathcal{R}_0$ with respect to key epidemiological parameters and control variables.

7.2. Global sensitivity via PRCCls

Local indices quantify sensitivity at a specific point in the parameter space, whereas global sensitivity assesses robustness under simultaneous variation of multiple parameters. We use PRCC, which measures the monotonic association between each input parameter and the output $\mathcal{R}_0$, while controlling for other parameters. The global uncertainty ranges are listed in Table 4, the PRCC results are reported in Table 5, and the overall PRCC ranking is shown in Figure 5.

To ensure reproducibility of the global sensitivity analysis, the LHS-PRCC computational workflow used to generate the PRCC values reported in Table 5 is summarized in Algorithm 1.

Table 4. Parameter ranges used for global sensitivity analysis.

Parameter	**Description**	**Range**	**Unit**
β_1	Transmission rate (unaware susceptible people)	$[0.10,\ 0.80]$	yr^{-1}
β_2	Transmission rate (aware susceptible people)	$[0.05,\ 0.50]$	yr^{-1}
ε	Relative infectiousness of diagnosed class	$[0.2,\ 0.9]$	–
τ_1	Baseline diagnosis (testing) rate	$[0.2,\ 2.5]$	yr^{-1}
τ_2	Baseline treatment-induced recovery rate	$[0.5,\ 6.0]$	yr^{-1}
γ_1	Hospitalization/linkage-to-care rate	$[0.1,\ 2.0]$	yr^{-1}
ξ_1	Natural/spontaneous recovery rate	$[0.05,\ 0.40]$	yr^{-1}
η_1	Disease-induced mortality (diagnosed)	$[0.0,\ 0.05]$	yr^{-1}
η_2	Disease-induced mortality (hospitalized)	$[0.0,\ 0.08]$	yr^{-1}
δ	Natural death rate	$[1/85,\ 1/60]$	yr^{-1}
u_1	Awareness control (fixed level for equilibrium analysis)	$[0,\ 1]$	–
u_2	Testing control (fixed level for equilibrium analysis)	$[0,\ 1]$	–
u_3	Treatment control (fixed level for equilibrium analysis)	$[0,\ 1]$	–

Table 5. PRCC-based global sensitivity of $\mathcal{R}_0$ using LHS ($M = 6000$) over Table 4.

Parameter	PRCC	p-value	Effect on $\mathcal{R}_0$
β_1	0.594	$< 10^{-16}$	Strong positive
β_2	0.681	$< 10^{-16}$	Strong positive
ε	0.244	$< 10^{-16}$	Moderate positive
τ_1	−0.598	$< 10^{-16}$	Strong negative
ξ_1	−0.477	$< 10^{-16}$	Moderate/strong negative
γ_1	−0.329	$< 10^{-16}$	Moderate negative
η_1	−0.027	3.33×10^{-2}	Very weak negative
δ	−0.017	1.90×10^{-1}	Not significant
u_1	−0.348	$< 10^{-16}$	Moderate negative
u_2	−0.702	$< 10^{-16}$	Strongest negative

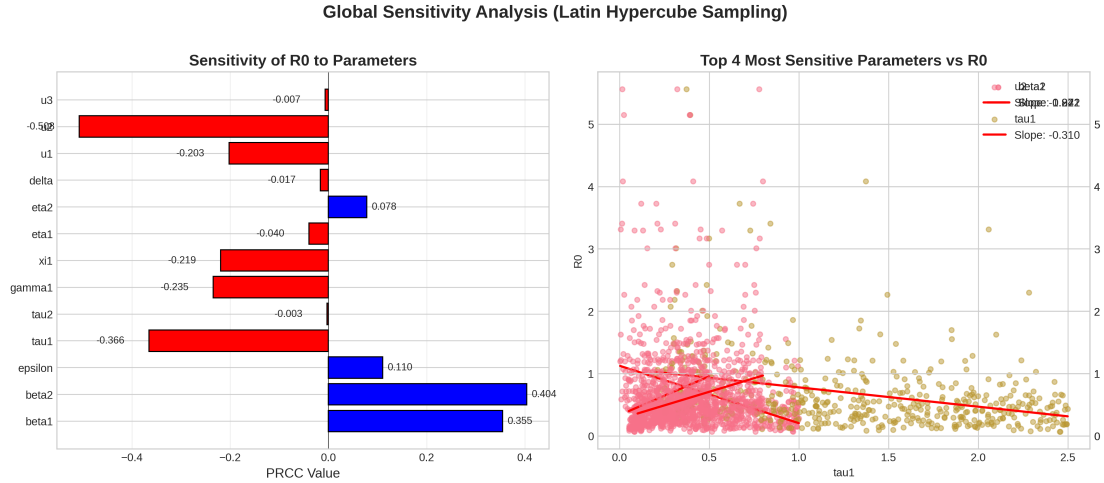

Figure 5. Global sensitivity analysis of $\mathcal{R}_0$ using PRCCs, highlighting the relative importance of transmission, testing, and awareness parameters.

Algorithm 1 LHS-PRCC analysis of $\mathcal{R}_0$

Require: Parameter ranges for $\Theta = (p_1, \ldots, p_m)$; sample size M; $\mathcal{R}_0$ formula (5.6).
Ensure: PRCC values and significance for all parameters.

Generate an $M \times m$ Latin hypercube sample $\{\Theta^{(j)}\}_{j=1}^{M}$ within the specified ranges.
for $j = 1$ to M **do**
  Compute (S_1^0, S_2^0).
  Compute $\mathcal{R}_0^{(j)}$.
end for
Rank-transform each parameter column and the output vector $\mathcal{R}_0$.
for $i = 1$ to m **do**
  Regress ranked p_i on ranked $\{p_k\}_{k \neq i}$; store residuals $\hat{r}_{p_i}$.
  Regress ranked $\mathcal{R}_0$ on ranked $\{p_k\}_{k \neq i}$; store residuals $\hat{r}_y$.
  Compute $\text{PRCC}_i = \text{corr}(\hat{r}_{p_i}, \hat{r}_y)$.
  Compute p-value for PRCC_i (optional).
end for
Report PRCCs and Table 5.

8. Center manifold bifurcation

In this section, we show that the system (2.1) undergoes a *transcritical bifurcation* at $\mathcal{R}_0 = 1$. Consequently, when $\mathcal{R}_0$ crosses 1 from below, a unique EE emerges and is locally asymptotically stable for $\mathcal{R}_0 > 1$ sufficiently close to 1.

8.1. Bifurcation parameter and critical point

Let μ be a bifurcation parameter chosen as one of the transmission parameters (e.g., $\mu = \beta_1$). Use μ^* the critical value such that

$$\mathcal{R}_0(\mu^*) = 1.$$

We write $\tilde{\mu} = \mu - \mu^*$, so that $\tilde{\mu} = 0$ corresponds to the bifurcation point. Let $\mathcal{E}_0$ denote the DFE.

8.2. Linearization at the DFE

Let $X = (S_1, S_2, U, I, H, R)^\top$ and write the model as

$$\dot{X} = F(X, \mu).$$

The Jacobian in DFE is $J_0 := D_X F(\mathcal{E}_0, \mu^*)$. The standard next-generation theory implies that, at $\mu = \mu^*$,

(1) J_0 has a *simple* eigenvalue at 0 (because $\mathcal{R}_0(\mu^*) = 1$);
(2) all other eigenvalues have strictly negative real parts.

Thus, the DFE is non-hyperbolic at μ^* and a center-manifold reduction applies.

8.3. Reduction to the infection-driving subspace

The only nonlinear infection mechanism is through the incidence term (standard incidence)

$$\alpha_1 S_1 + \alpha_2 S_2 = \frac{\beta_1 S_1 + \beta_2 S_2}{N}(U + \varepsilon I), \qquad N = S_1 + S_2 + U + I + H + R.$$

Hence, the local bifurcation is governed by the infected variables (U, I) (the class H does not correspond to the incidence in (2.1)). For center manifold calculations, we keep the full state, but only the second derivatives arising from the incidence contribute to the bifurcation coefficients.

8.4. Right and left eigenvectors at $\tilde{\mu} = 0$

Let w be the right eigenvector and v the left eigenvector associated with the zero eigenvalue of J_0:

$$J_0 w = 0, \qquad v^\top J_0 = 0, \qquad v^\top w = 1.$$

Because the infection subsystem at the DFE is (up to a stable H-direction) driven by (U, I), we may take w and v to have support on the infected coordinates, i.e.,

$$w = (w_{S_1}, w_{S_2}, w_U, w_I, w_H, w_R)^\top, \qquad v = (0, 0, v_U, v_I, 0, 0)^\top,$$

with $w_U > 0$, $w_I > 0$, $v_U > 0$, $v_I > 0$.

From the infected linearization at the DFE,

$$\dot{U} = k(U + \varepsilon I) - k_U U, \qquad \dot{I} = \tau_1 u_2 U - k_I I,$$

where

$$k = \frac{\beta_1 S_1^0 + \beta_2 S_2^0}{N^0}, \quad k_U = \tau_1 u_2 + \xi_1 + \delta, \quad k_I = \gamma_1 + \eta_1 + \xi_1 + \delta, \quad N^0 = \frac{A}{\delta},$$

one convenient choice of eigenvectors (up to scaling) is

$$w_U = 1, \qquad w_I = \frac{\tau_1 u_2}{k_I}, \qquad w_H = \frac{\gamma_1}{k_H} w_I, \qquad w_R = \frac{1}{\delta}\Big(\xi_1(1 + w_I) + \tau_2 u_3\, w_H\Big), \tag{8.1}$$

and w_{S_1}, w_{S_2} are determined by the linear constraints induced by the susceptible equations on the center manifold (their explicit closed forms are not needed for the sign of the bifurcation coefficients). The left eigenvector components can be chosen so that

$$v_I = \frac{k\varepsilon}{k_I}\, v_U, \qquad v_U > 0, \qquad \text{and} \qquad v^\top w = 1. \tag{8.2}$$

8.5. Bifurcation coefficients

Following the theorem in [19], define

$$a = \sum_{k=1}^{6}\sum_{i=1}^{6}\sum_{j=1}^{6} v_k w_i w_j \frac{\partial^2 f_k}{\partial x_i \partial x_j}(\mathcal{E}_0, \mu^*), \qquad b = \sum_{k=1}^{6}\sum_{i=1}^{6} v_k w_i \frac{\partial^2 f_k}{\partial x_i \partial \mu}(\mathcal{E}_0, \mu^*), \tag{8.3}$$

where f_k is the k-th component of $F(X, \mu)$.

Key observation. All second derivatives in (8.3) vanish except those coming from the incidence term in the U-equation. In particular, only $k = U$ contributes, so

$$a = v_U \sum_{i,j} w_i w_j \frac{\partial^2 f_U}{\partial x_i \partial x_j}(\mathcal{E}_0, \mu^*), \qquad b = v_U \sum_{i} w_i \frac{\partial^2 f_U}{\partial x_i \partial \mu}(\mathcal{E}_0, \mu^*).$$

8.6. Sign of b (transversality)

Take $\mu = \beta_1$. Near the DFE,

$$f_U = \frac{\beta_1 S_1 + \beta_2 S_2}{N}(U + \varepsilon I) - k_U U.$$

Thus

$$\frac{\partial^2 f_U}{\partial \beta_1 \partial U}\Big|_{\varepsilon_0} = \frac{S_1^0}{N^0} > 0, \qquad \frac{\partial^2 f_U}{\partial \beta_1 \partial I}\Big|_{\varepsilon_0} = \varepsilon \frac{S_1^0}{N^0} > 0,$$

and all other mixed derivatives with β_1 vanish at the DFE. Hence, we have

$$b = v_U \left(w_U \frac{S_1^0}{N^0} + w_I\, \varepsilon \frac{S_1^0}{N^0} \right) = v_U \frac{S_1^0}{N^0}(w_U + \varepsilon w_I) > 0. \tag{8.4}$$

8.7. Sign of a (nonlinear saturation due to standard incidence)

The nonlinearity arises primarily from the factor $1/N$ in the standard incidence. Expanding around the DFE, we have

$$\frac{1}{N} = \frac{1}{N^0} - \frac{N - N^0}{(N^0)^2} + O(\|X - \mathcal{E}_0\|^2),$$

and in the center manifold $N - N^0$ contains a positive contribution from infected coordinates in the direction w (notably U, I, H, R in (8.1)). This produces a *negative* quadratic term in the U-equation, giving $a < 0$.

More explicitly, one obtains the dominant contribution

$$a = -2v_U \frac{\beta_1^* S_1^0 + \beta_2 S_2^0}{(N^0)^2} (w_U + \varepsilon w_I)(w_U + w_I + w_H + w_R) \; + \; \text{(additional nonpositive terms)}, \tag{8.5}$$

and therefore

$$a < 0,$$

since all factors are positive and the remaining quadratic contributions from the susceptible adjustments on the center manifold are nonpositive for standard incidence.

8.8. Conclusion: Forward bifurcation

Theorem 8 (Forward transcritical bifurcation at $\mathcal{R}_0 = 1$)**.** *Assume all parameters are positive and let $\mu = \beta_1$ be the bifurcation parameter. At $\mu = \mu^*$ such that $\mathcal{R}_0(\mu^*) = 1$, the model undergoes a forward (transcritical) bifurcation. In particular,*

(1) If $\mathcal{R}_0 < 1$, the DFE $\mathcal{E}_0$ is locally asymptotically stable;
(2) If $\mathcal{R}_0 > 1$ and sufficiently close to 1, there is a unique EE $\mathcal{E}^*$ near $\mathcal{E}_0$ which is locally asymptotically stable.

Proof. At $\mu = \mu^*$, J_0 has a simple zero eigenvalue and all remaining eigenvalues have negative real parts. The center manifold theorem applies. By (8.4), $b > 0$ (transversality). By (8.5), $a < 0$. Therefore, by the Castillo-Chavez and Song bifurcation theorem, the system exhibits a forward transcritical bifurcation at $\mathcal{R}_0 = 1$ and the EE emerging for $\mathcal{R}_0 > 1$ is locally asymptotically stable. □

The transcritical bifurcation structure near $\mathcal{R}_0$ is depicted in Figure 6. Figure 6 illustrates the transcritical bifurcation structure of the HCV transmission model with respect to a key transmission parameter. As the basic reproduction number crosses the critical threshold $\mathcal{R}_0 = 1$, the DFE loses stability and a unique EE emerges smoothly, confirming the analytical results obtained by center manifold theory.

Remark 4. *The same conclusion holds if one chooses $\mu = \beta_2$ (or another transmission-related parameter) as the bifurcation parameter, provided $\frac{\partial \mathcal{R}_0}{\partial \mu}\Big|_{\mu=\mu^*} \neq 0$.*

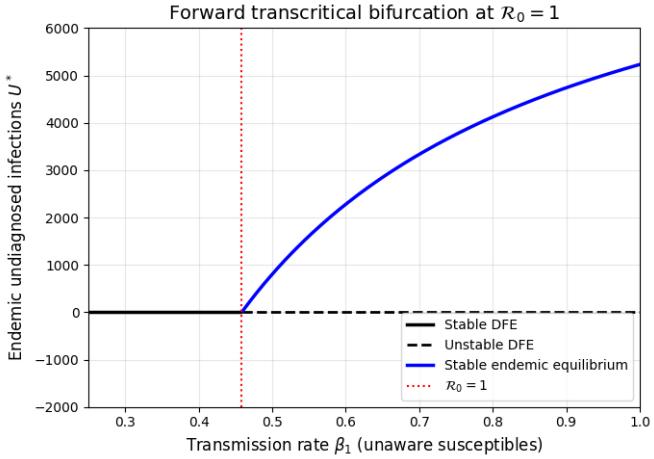

Figure 6. Bifurcation diagram of the endemic infection level with respect to a transmission parameter, indicating a forward (transcritical) bifurcation at $\mathcal{R}_0 = 1$.

9. Numerical results

The parameter values in Table 6 are chosen within the biologically plausible ranges reported in the literature on HCV transmission and are used to validate the analytical results. These values are not claimed to be calibrated to a specific population, but are sufficient to demonstrate the consistency between theoretical predictions and numerical dynamics. When epidemiological data are available, the same framework can be recalibrated using data-driven estimation techniques.

Table 6. Baseline parameter values used for numerical validation of system (2.1).

Parameter	Description	Value	Unit	Ref.
A	Recruitment rate into population	1.0×10^4	persons yr^{-1}	
δ	Natural death rate	$1/70$	yr^{-1}	[1]
β_1	Transmission rate (unaware susceptible people)	0.45	yr^{-1}	
β_2	Transmission rate (aware susceptible people)	0.20	yr^{-1}	
ε	Relative infectiousness of diagnosed class	0.5	dimensionless	
τ_1	Diagnosis (testing) rate	1.2	yr^{-1}	
τ_2	Treatment-induced recovery rate	2.0	yr^{-1}	
γ_1	Hospitalization rate	0.6	yr^{-1}	
ξ_1	Natural recovery rate	0.15	yr^{-1}	
η_1	Disease-induced death (diagnosed)	0.01	yr^{-1}	
η_2	Disease-induced death (hospitalized)	0.015	yr^{-1}	
u_1	Media awareness control level	0.4	–	Assumed
u_2	Diagnostic testing control level	0.5	–	Assumed
u_3	Treatment control level	0.6	–	Assumed

The baseline parameter values are used for theoretical and exploratory numerical analysis, which does not require calibration to any specific country or region or risk population. The numerical

comparisons should be understood as model-based qualitative displays of intervention effects, rather than population-specific quantitative predictions. The baseline values in Table 6 were selected using three principles: Standard demographic approximations for the natural mortality rate; biologically plausible values within the admissible parameter intervals listed in Table 4 for epidemiological transition parameters; and illustrative baseline intervention levels for control variables. The present study uses these values as reference standards for researchers to evaluate their findings, as they do not need to match actual surveillance data.

The baseline values used for numerical validation are provided in Table 6, and the resulting state trajectories are shown in Figure 7. Figure 7 presents the time evolution of all epidemiological compartments under the set of baseline parameters. The simulations verify the positivity and boundedness of the solutions and demonstrate convergence towards disease-free equilibrium when $\mathcal{R}_0 < 1$, in agreement with the theoretical stability analysis.

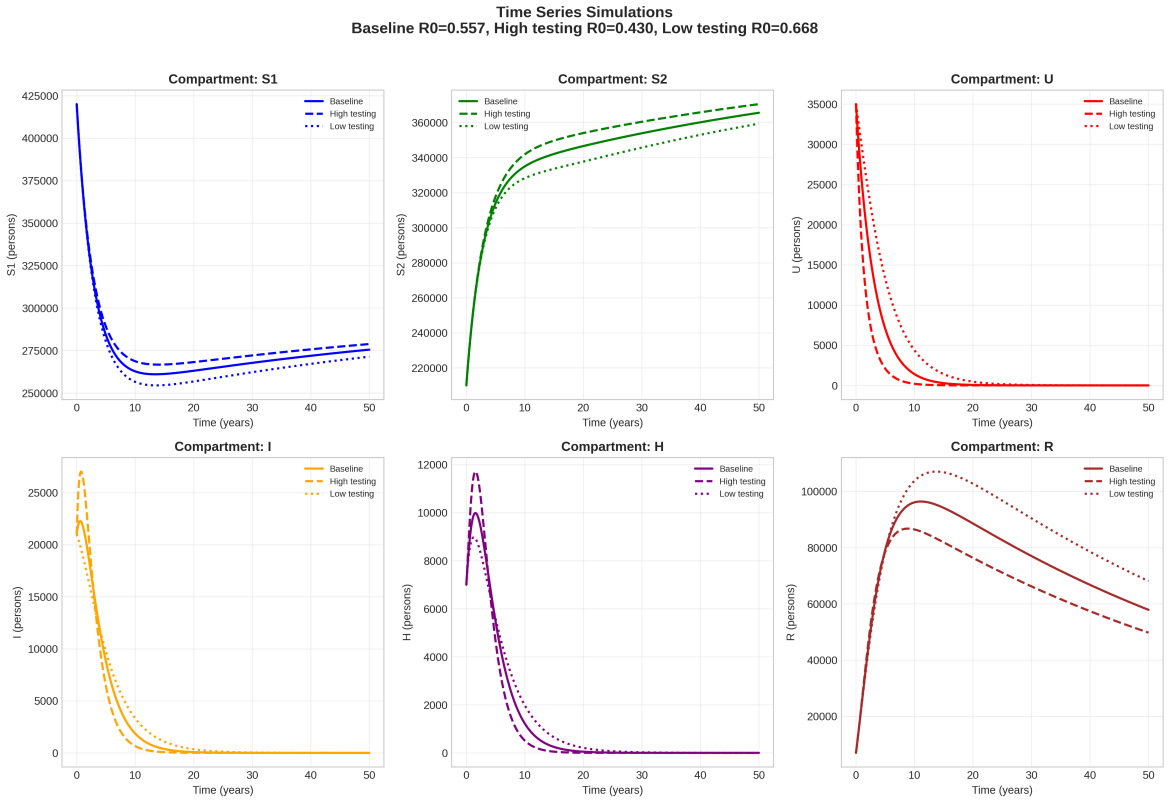

Figure 7. Time evolution of model compartments under baseline parameter values, demonstrating positivity and long-term boundedness of solutions.

To provide more specific policy guidance, we performed a comparative scenario-based analysis of combined intervention strategies involving awareness control (u_1), diagnostic testing control (u_2), and treatment control (u_3). Although the sensitivity and PRCC results identify the most influential individual controls on the basic reproduction number R_0, policy design in practice often requires comparing intervention *packages* rather than isolated parameters. Therefore, we examine how different combinations of awareness, testing, and treatment perform in epidemiological settings with varying initial prevalence levels.

Since the numerical experiments in this study are intended for theoretical validation rather than direct calibration to a specific population, we define prevalence scenarios operationally using the initial values of the infected compartments. Specifically, we consider:

$$\text{Low-prevalence scenario: } (U(0), I(0), H(0)) = (50, 20, 10);$$
$$\text{Moderate-prevalence scenario: } (U(0), I(0), H(0)) = (300, 120, 60);$$
$$\text{High-prevalence scenario: } (U(0), I(0), H(0)) = (1000, 400, 200).$$

The remaining compartments were adjusted to maintain the total initial population within the feasible region, and all other model parameters were fixed to the baseline values given in Table 6.

To compare policy-relevant intervention packages, we selected five representative strategies in Table 7.

Table 7. Combined intervention strategies considered for comparative policy analysis under different prevalence scenarios.

Strategy	u_1	u_2	u_3	**Interpretation**
A	0.8	0.3	0.5	Awareness-dominant control with high behavioral prevention, limited testing expansion, and moderate treatment support
B	0.3	0.8	0.5	Testing-dominant control emphasizing rapid case detection and moderate treatment support
C	0.5	0.5	0.8	Treatment-dominant control with balanced prevention and enhanced recovery support
D	0.8	0.8	0.8	Fully integrated high-intensity control strategy
E	0.2	0.2	0.8	Low-prevention strategy with treatment emphasis

In all prevalence scenarios, strategy D performs best because it reduces susceptibility, shortens the duration of undiagnosed infection, and allows recovery the first time. The approach highlights a hierarchy of interventions by prevalence: Testing-led strategies prove very efficient for containment in the early stages of awareness-led strategies, which, on the other hand, would be highly preferable in already moderately established epidemics. Finally, in settings where simultaneous reductions in transmission and/or clinical burden are required, the fully integrated intervention package is considered the most appropriate.

10. Discussion and policy implications

This study provides a policy-supported mathematical framework for examining the interactions among awareness, testing, and treatment in the dynamics of HCV transmission. By integrating behavioral awareness (u_1), diagnostic testing (u_2), and treatment control (u_3) into a compartmental model, we establish explicit analytical links between public health interventions and epidemic thresholds, the long-term persistence of the disease, and the feasibility of control.

The analytical derivation of the basic reproduction number $\mathcal{R}_0$ reveals that elimination of HCV is fundamentally governed by three interacting mechanisms: (i) Effective transmission intensity among susceptible subgroups, (ii) average duration of undiagnosed infection, and (iii) residual infectiousness after diagnosis. The forward (transcritical) bifurcation at $\mathcal{R}_0 = 1$ serves as a threshold separating local

disease extinction from disease persistence. In the present study, the local asymptotic stability of the DFE is analytically demonstrated for $\mathcal{R}_0 < 1$ while numerical simulations indicate convergence toward the disease-free state for the representative parameter regimes examined.

From a policy perspective, under the present model, the qualitative threshold condition for disease elimination is $\mathcal{R}_0 < 1$. The threshold and sensitivity analyses show that $\mathcal{R}_0$ must be decreased below one to successfully eliminate the disease, while the numerical simulations demonstrate that the disease-free state can be reached at all conditions of the tested parameters. Sensitivity and PRCC analyses demonstrate a strong hierarchy among control levers. The transmission parameters β_1 and β_2 remain the dominant drivers of $\mathcal{R}_0$, underscoring the importance of reducing behavioral risk. However, among controllable interventions, diagnostic testing (u_2) emerges as the most influential lever for reducing $\mathcal{R}_0$, followed by awareness campaigns (u_1).

This hierarchy is clearly illustrated in Figure 8, which shows that increases in testing intensity lead to rapid reductions in undiagnosed infections and overall transmission potential, even when treatment coverage is moderate. Awareness interventions indirectly reduce transmission by shifting individuals from high-risk unaware susceptibility to lower-risk aware susceptibility, producing a substantial population-level effect.

A key policy insight from this study is that the treatment control (u_3) does not appear explicitly in $\mathcal{R}_0$. This does not diminish the importance of treatment; rather, it clarifies its role. Treatment primarily reduces the disease's burden, prevalence, and morbidity by shortening the infectious period and accelerating recovery, as illustrated in Figure 9. However, when hospitalized individuals do not directly contribute to new infections, treatment alone cannot interrupt transmission.

This finding aligns with current WHO strategies emphasizing the integration of testing and treatment: Testing reduces transmission by shortening the undiagnosed infectious period, while treatment consolidates these gains by lowering prevalence and preventing complications. From a policy standpoint, treatment should therefore be viewed as a burden-reduction and sustainability tool, rather than a stand-alone elimination strategy.

The optimal control simulations in Figure 9 further emphasize the need for coordinated intervention strategies. Pareto front analysis indicates that aggressive early investment in testing yields the largest marginal reductions in infections, after which awareness and treatment interventions provide diminishing but stabilizing returns. This is directly relevant in resource-limited settings, where budgets for HCV elimination are constrained. The exploratory scenarios demonstrate that testing is the most effective method to reduce transmission potential, while awareness and treatment provide additional benefits. The intervention assessment provides medical professionals with a qualitative method to determine which interventions offer the most effective treatment options.

For national elimination programs, particularly in low and middle-income countries, the model supports a phased strategy: (i) Rapid expansion of tests to reduce $\mathcal{R}_0$ below unity, (ii) sustained awareness campaigns to maintain behavioral change, and (iii) long-term treatment programs to minimize disease burden and prevent resurgence. The mathematical robustness of the results—validated through global stability and bifurcation analysis—ensures that these conclusions are not artifacts of specific parameter choices.

Although the model captures essential features of HCV transmission and control, it does not explicitly incorporate the risk of reinfection, heterogeneous risk networks, or spatial structure. The study results should be interpreted as qualitative insights from the model, given the lack of calibration

to specific population groups and health systems, as well as the testing of specific surveillance data. The proposed transmission structure model demonstrates its primary value by showing how awareness, testing, and treatment interact. Future extensions could integrate data-driven calibration, age- or risk-stratified mixing, and stochastic effects to improve policy precision. However, the present framework provides a transparent and an analytically grounded foundation for evidence-based HCV control planning.

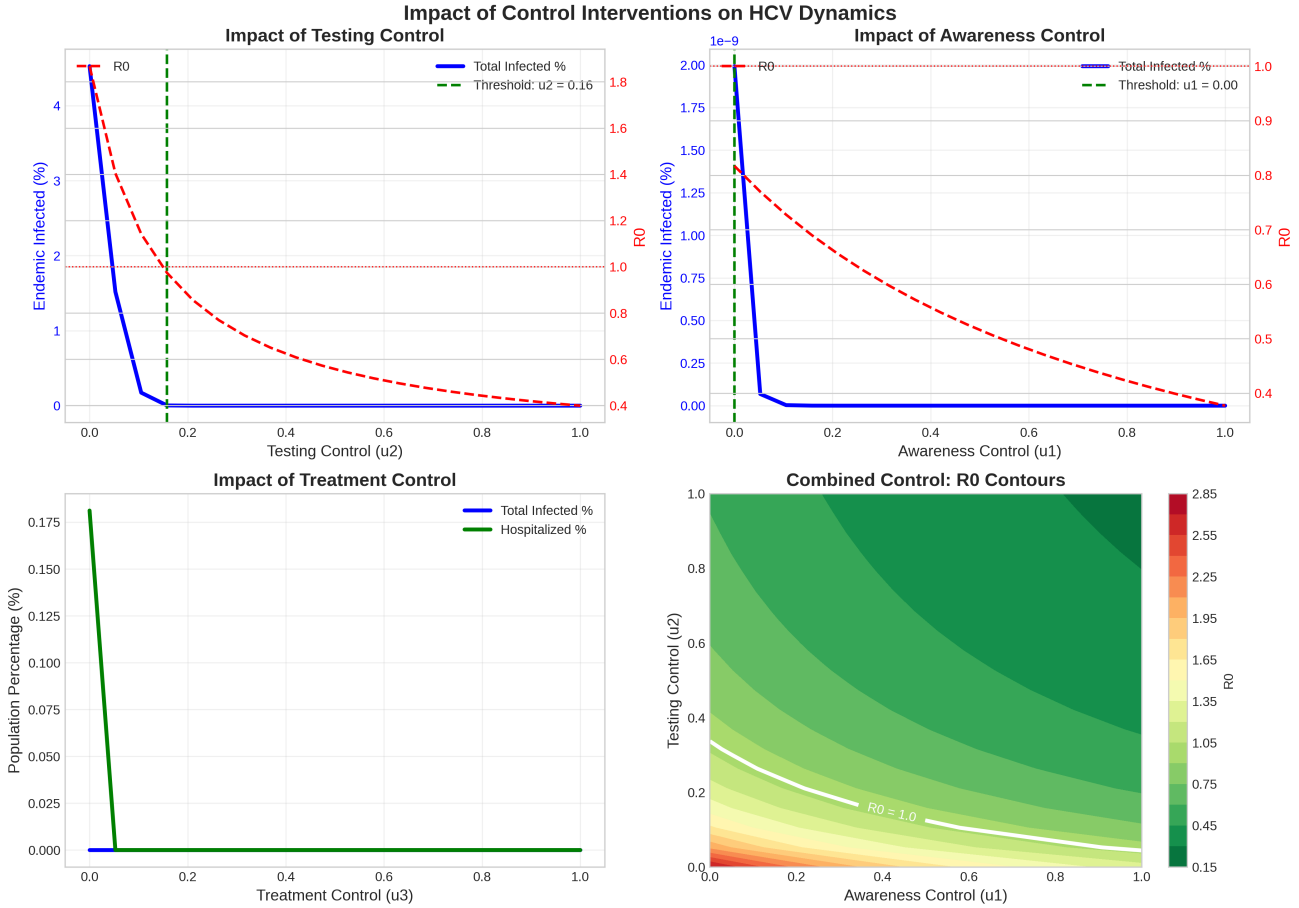

Figure 8. Impact of control interventions on HCV dynamics. The panels illustrate the effects of diagnostic testing (u_2), awareness campaigns (u_1), and treatment coverage (u_3) on key epidemiological outcomes. Increased testing rapidly reduces the undiagnosed infected population and overall transmission, while awareness lowers susceptibility by shifting individuals into lower-risk behavioral states. Treatment primarily reduces disease burden by accelerating recovery and lowering prevalence, but does not directly alter the $\mathcal{R}_0$.

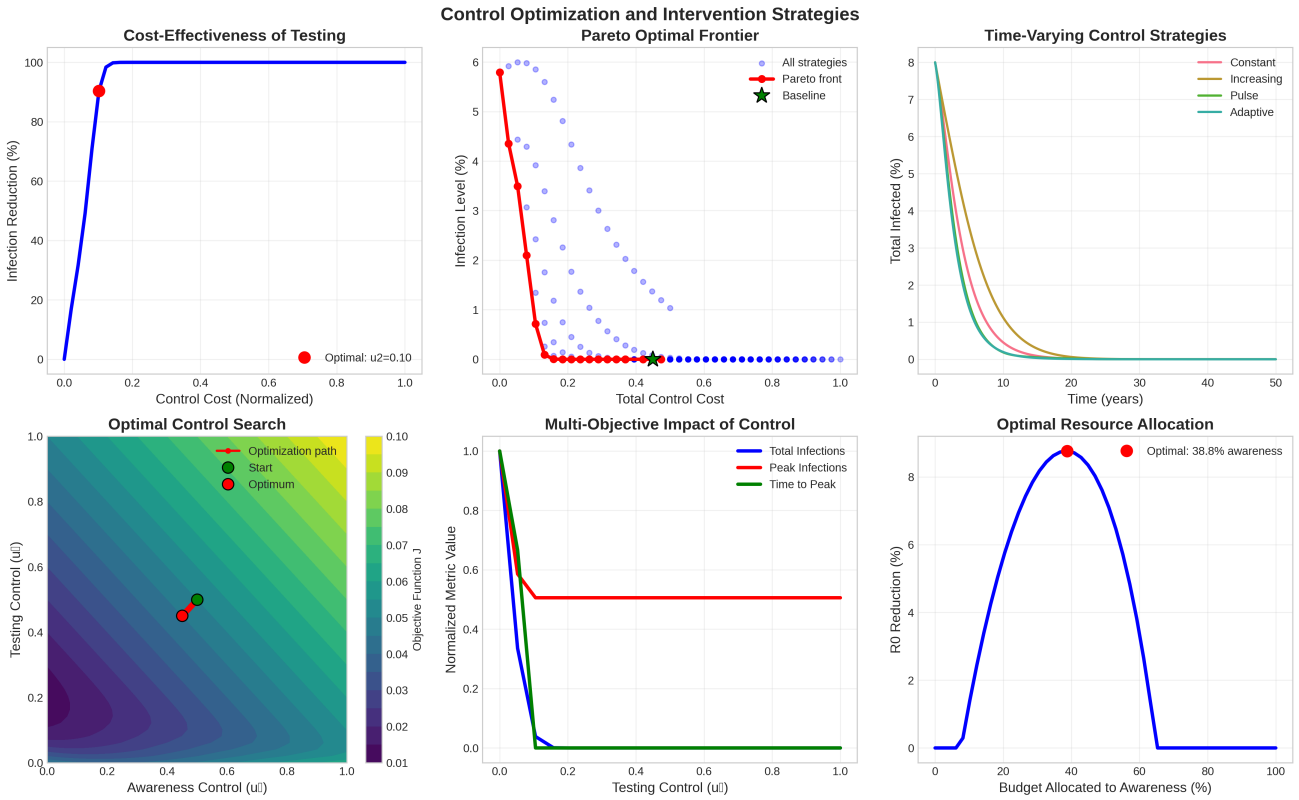

Figure 9. Optimal control and intervention trade-offs for HCV elimination. Panels show cost-effectiveness of testing, Pareto-optimal intervention fronts, time-dependent optimal control strategies, and optimal resource allocation under budget constraints. The results indicate that prioritizing diagnostic testing yields the largest marginal reduction in infections, while awareness and treatment interventions provide complementary long-term stabilization.

11. Conclusions

We established a calibration process for our study using a deterministic compartmental model that simulates HCV transmission based on three factors: People who know about the disease, diagnostic testing, and treatment programs. The model demonstrated mathematical validity, enabling researchers to derive an explicit formula for the basic reproduction number $\mathcal{R}_0$ to distinguish between disease elimination and disease persistence.

The research provides qualitative evidence on HCV transmission patterns, which governmental awareness efforts, testing programs, and treatment methods work together to develop the proposed framework. The model demonstrates that diagnostic testing and awareness are the two most effective methods for reducing transmission rates, while treatment reduces disease severity. The analysis results must be treated as theoretical research because they do not focus on specific population groups, yet they provide guidance for future population-based research and policy development.

In summary, the model establishes a mathematically valid approach to investigate HCV transmission patterns which result from public awareness and testing and treatment programs. The autonomous system with fixed control levels has been analyzed using rigorous methods, which demonstrate its positivity and boundedness, as well as the existence of a DFE, a basic reproduction

number, and local stability of the DFE and one EE, which appears when $\mathcal{R}_0 > 1$. The manuscript derives a conditional local stability criterion for the EE using the Routh-Hurwitz conditions, which researchers have tested using typical parameter sets rather than providing a universal proof. The theory is supported by sensitivity and scenario analyses that show how the key parameters affect treatment outcomes across different parameter ranges.

Author contributions

Debnarayan Khatua: Conceptualization, data curation, methodology, project administration, validation, visualization, writing–original draft; Bapin Mondal: Conceptualization, validation, visualization, supervision, writing–review & editing; Md Sadikur Rahman: Investigation, project administration, resources, Supervision, writing–review & editing; Sadiah M. Aljeddani: Formal analysis, funding acquisition, software, writing–review & editing.

Use of Generative AI tools declaration

The authors declare they have not used artificial intelligence (AI) tools in the creation of this article.

Funding

This research work was funded by Umm Al-Qura University, Saudi Arabia under grant number: 26UQU4310037GSSR06.

Acknowledgements

The authors extend their appreciation to Umm Al-Qura University, Saudi Arabia for funding this research work through grant number: 26UQU4310037GSSR06.

Conflict of interest

No conflict of interest.

References

1. World Health Organization, *Global progress report on HIV, viral hepatitis and sexually transmitted infections, 2021: accountability for the global health sector strategies 2016–2021: actions for impact*, Geneva: WHO publications, 2021.
2. R. Chien, M. Hsu, Y. Luo, C. Liu, L. Lin, S. Wei, et al., Current status of HCV elimination in taiwan, *J. Formos. Med. Assoc.*, **124** (2025), S90–S95. https://doi.org/10.1016/j.jfma.2025.09.031
3. K. Sharma, M. K. Murthy, A review of historical landmarks and pioneering technologies for the diagnosis of hepatitis C virus (HCV), *Eur. J. Clin. Microbiol. Infect. Dis.*, **44** (2025), 1289–1303. https://doi.org/10.1007/s10096-025-05110-y

4. World Health Organization, Viral hepatitis: fact sheet on sustainable development goals (SDGs): health targets, WHO/EURO: 2017-2389-42144-58061.
5. R. L. Fleurence, H. J. Alter, F. S. Collins, J. W. Ward, Global elimination of hepatitis C virus, *Annu. Rev. Med.*, **76** (2025), 29–41. https://doi.org/10.1146/annurev-med-050223-111239
6. *World Health Organization, WHO publishes updated guidance on hepatitis C infection—with new recommendations on treatment of adolescents and children, simplified service delivery and diagnostics*, WHO, 2022. Available from: `https://www.who.int/news/item/24-06-2022-WHO-publishes-updated-guidance-on-hepatitis-C-infection`.
7. G. Steffen, A. Krings, S. Guttmann, N. Lübke, K. Meyer-Schlinkmann, C. Tiemann, et al., Progress and challenges in the elimination of hepatitis C among people who inject drugs in germany: results of a pilot study for a national monitoring system, 10 years after the first data collection, *Harm Reduct. J.*, **21** (2024), 222. https://doi.org/10.1186/s12954-024-01119-2
8. M. Sallam, R. Khalil, Contemporary insights into hepatitis C virus: a comprehensive review, *Microorganisms*, **12** (2024), 1035. https://doi.org/10.3390/microorganisms12061035
9. H. J. Wu, S. T. Shih, T. L. Applegate, J. A. Kwon, E. B. Cunningham, J. Grebely, et al., Impact of simplified HCV diagnostic strategies on the HCV epidemic among men who have sex with men in the era of hiv oral pre-exposure prophylaxis in taiwan: a modelling study, *J. Int. AIDS Soc.*, **27** (2024), e26251. https://doi.org/10.1002/jia2.26251
10. J. L. Calleja, J. Espin, A. Kaushik, M. Hernandez-Guerra, R. Blissett, A. Yehoshua, et al., The efficiency of increased HCV testing and treatment strategies in spain to achieve elimination goals, *PharmacoEcon.-Open*, **8** (2024), 221–233. https://doi.org/10.1007/s41669-023-00458-3
11. A. B. Pitcher, A. Borquez, B. Skaathun, N. K. Martin, Mathematical modeling of hepatitis C virus (HCV) prevention among people who inject drugs: a review of the literature and insights for elimination strategies, *J. Theor. Biol.*, **481** (2019), 194–201. https://doi.org/10.1016/j.jtbi.2018.11.013
12. E. Tatara, A. Gutfraind, N. T. Collier, D. Echevarria, S. J. Cotler, M. E. Major, et al., Modeling hepatitis c micro-elimination among people who inject drugs with direct-acting antivirals in metropolitan chicago, *PLoS One*, **17** (2022), e0264983. https://doi.org/10.1371/journal.pone.0264983
13. B. Mondal, N. Sk, S. Acharya, Dynamics of ebola virus disease with awareness effects: a case study of guinea and sierra leone, *Nonlinear Dyn.*, **113** (2025), 22021–22042. https://doi.org/10.1007/s11071-025-11286-x
14. A. Yeung, N. E. Palmateer, J. F. Dillon, S. A. McDonald, S. Smith, S. Barclay, et al., Population-level estimates of hepatitis c reinfection post scale-up of direct-acting antivirals among people who inject drugs, *J. Hepatol.*, **76** (2022), 549–557. https://doi.org/10.1016/j.jhep.2021.09.038
15. A. Artenie, A. Trickey, K. J. Looker, J. Stone, A. G. Lim, H. Fraser, et al., Global, regional, and national estimates of hepatitis C virus (HCV) infection incidence among people who inject drugs and number of new annual HCV infections attributable to injecting drug use: a multi-stage analysis, *Lancet Gastroenterol.*, **10** (2025), 315–331. https://doi.org/10.1016/S2468-1253(24)00442-4

16. L. Zhu, J. R. Havens, A. E. Rudolph, A. M. Young, G. E. Yazdi, W. W. Thompson, et al., Hepatitis C virus transmission among people who inject drugs in rural united states: mathematical modeling study using stochastic agent-based network simulation, *Am. J. Epidemiol.*, **195** (2026), 937–947. https://doi.org/10.1093/aje/kwaf052

17. Z. Ward, R. Simmons, H. Fraser, A. Trickey, J. Kesten, A. Gibson, et al., Impact and cost-effectiveness of scaling up HCV testing and treatment strategies for achieving HCV elimination among people who inject drugs in england: a mathematical modelling study, *The Lancet Regional Health: Europe*, **49** (2025), 101176. https://doi.org/10.1016/j.lanepe.2024.101176

18. P. Van den Driessche, J. Watmough, Reproduction numbers and sub-threshold endemic equilibria for compartmental models of disease transmission, *Math. Biosci.*, **180** (2002), 29–48. https://doi.org/10.1016/S0025-5564(02)00108-6

19. C. Castillo-Chavez, B. Song, Dynamical models of tuberculosis and their applications, *Math. Biosci. Eng.*, **1** (2004), 361–404.

20. S. Marino, I. B. Hogue, C. J. Ray, D. E. Kirschner, A methodology for performing global uncertainty and sensitivity analysis in systems biology, *J. Theor. Biol.*, **254** (2008), 178–196. https://doi.org/10.1016/j.jtbi.2008.04.011

21. A. Saltelli, S. Tarantola, F. Campolongo, M. Ratto, *Sensitivity analysis in practice: a guide to assessing scientific models*, Hoboken: John Wiley & Sons, Ltd, 2004. https://doi.org/10.1002/0470870958

22. B. Kumar, M. K. Singh, D. Khatua, A. De, Understanding HCV through the lens of mathematical modeling: a comprehensive review, *Journal of Applied Nonlinear Dynamics*, **13** (2024), 761–780. https://doi.org/10.5890/JAND.2024.12.010

AIMS Press